

Chemical Looping Technology – Reaction, Reactor and Solids Flow Issues

by

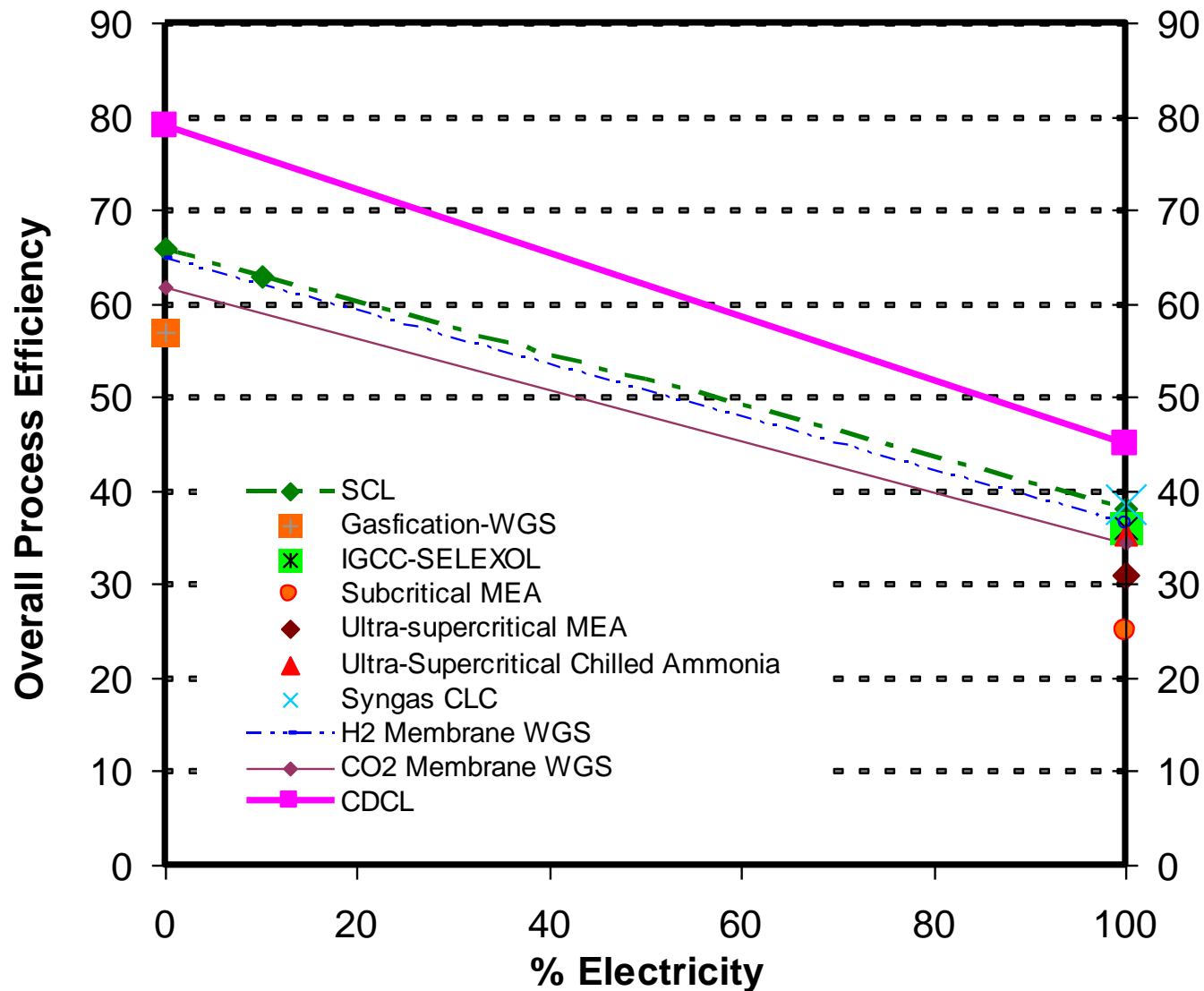
L. S. Fan

**Department of Chemical and Biomolecular
Engineering**

**The Ohio State University
Columbus, Ohio 43210**

August 17, 2011

Comparison Among Gaseous Chemical Looping, Direct Coal Chemical Looping and Traditional Coal to Hydrogen/Electricity Processes



Assumptions used are similar to those adopted by the USDOE baseline studies.

Aspen Plus[®] Modeling Results

	Base Plant	MEA Plant	CDCL Plant
Coal Feed, kg/h (lb/h)	198,391 (437,378)	278,956 (614,994)	210,118 (463,231)
CO ₂ Emissions, kg/MWh _{net} (lb/MWh _{net})	856 (1,888)	121 (266)	~0 (~0)
CO ₂ Capture Efficiency, %	0	90	~100
Solid Waste, ^a kg/MWh _{net} (lb/MWh _{net})	35 (77)	49 (108)	39 (87)
Net Power Output, MW _e	550	550	550
Net Plant HHV Heat Rate, kJ/kWh (Btu/kWh)	9,788 (9,277)	13,764 (13,046)	10,357 (9,817)
Net Plant HHV Efficiency, %	36.8	26.2	34.8
Energy Penalty, ^b %	-	29	5

^aExcludes gypsum from wet FGD. ^bRelative to Base Plant; includes energy for CO₂ compression.

Topics

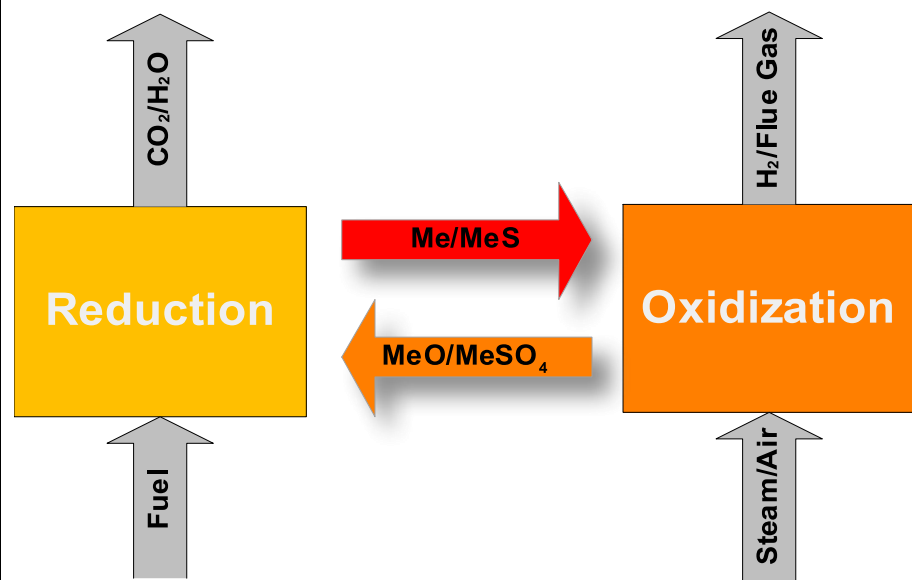
- Two Types of Chemical Looping Systems
- Particle Synthesis and Ionic Diffusion Mechanism
- Modes of Reactor Operation
- Stability of Solids Flow
- Chemical Looping System Efficiency
- Commercialization Potential

Chemical Looping for Fossil Fuel Conversions

Two typical types of looping reaction systems

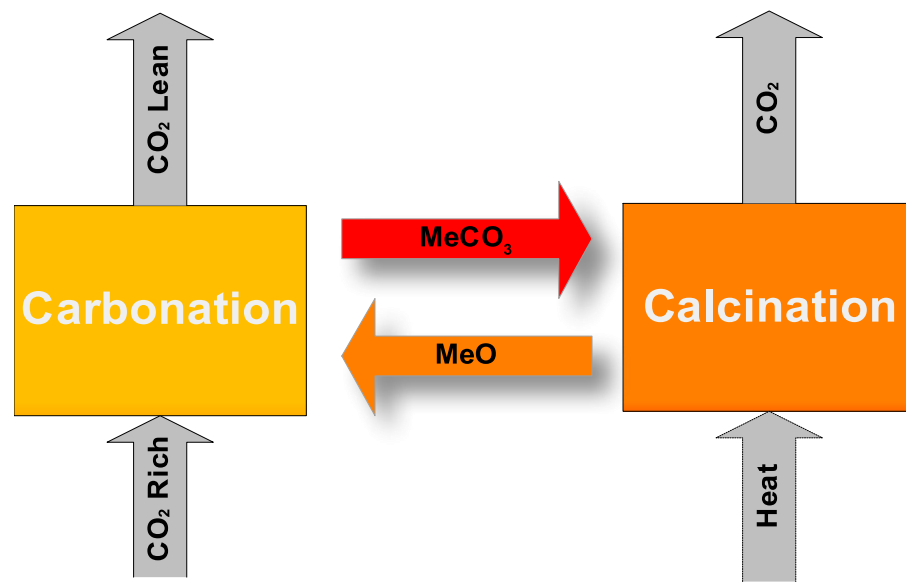
Oxygen Carrier (Type I)

Me/MeO, MeS/MeSO₄



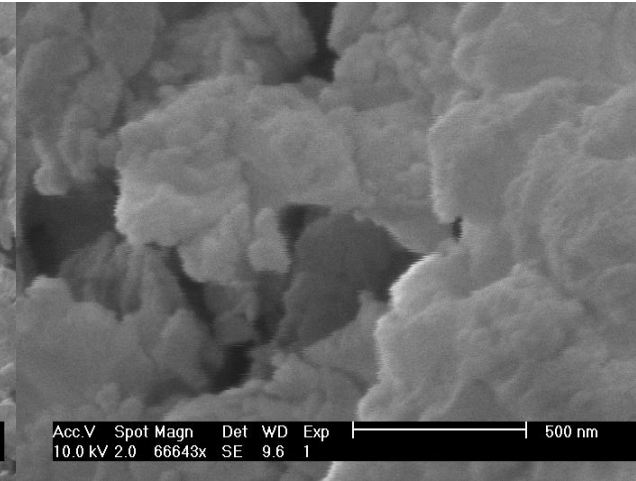
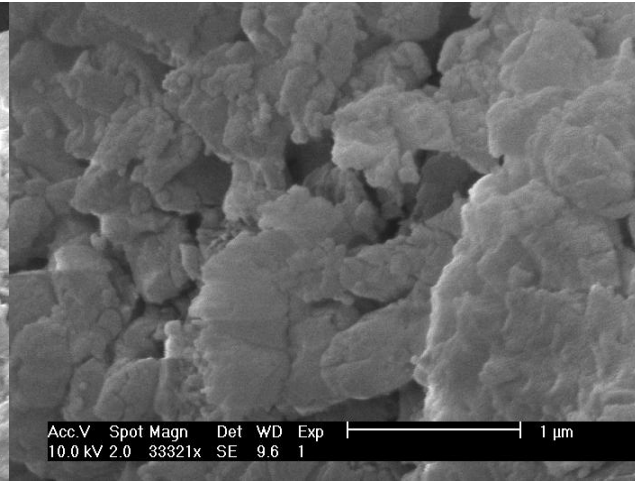
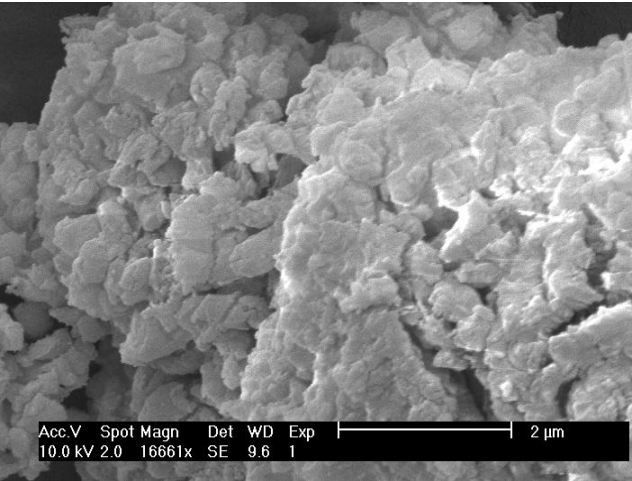
CO₂ Carrier (Type II)

MeO/MeCO₃

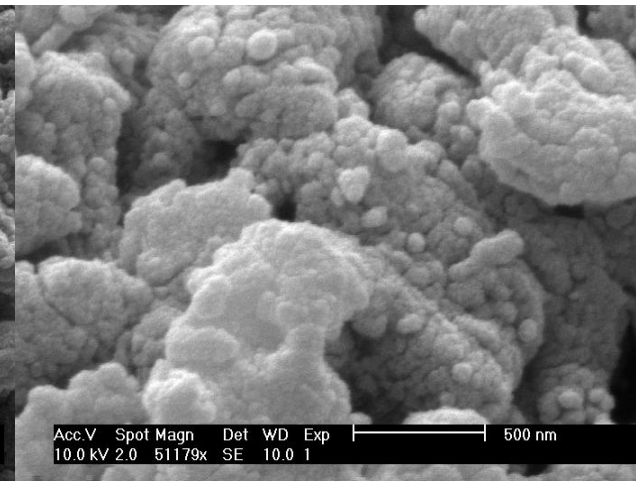
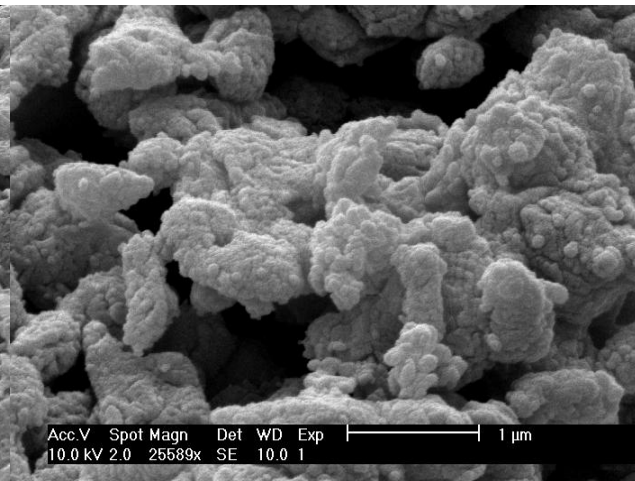
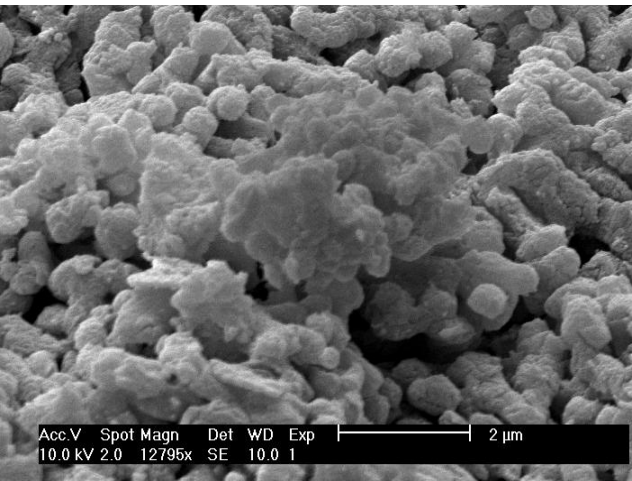


Macroscopic Properties of Calcium Oxide

Sintered_CaO



Hydrated_CaO



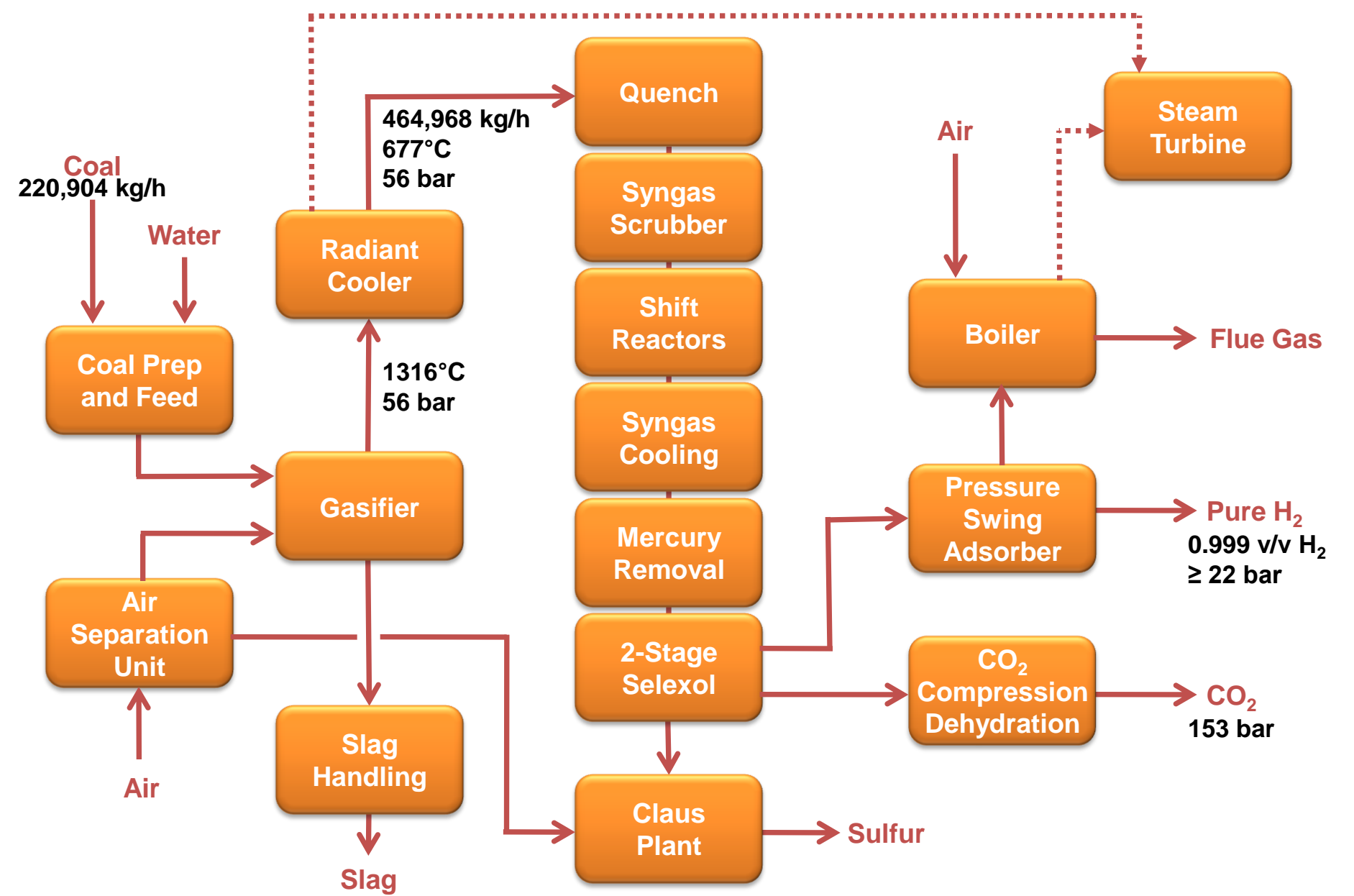
- Hydrated_CaO has smaller particles size
- Hydration caused cracks on the surface

[illegible]

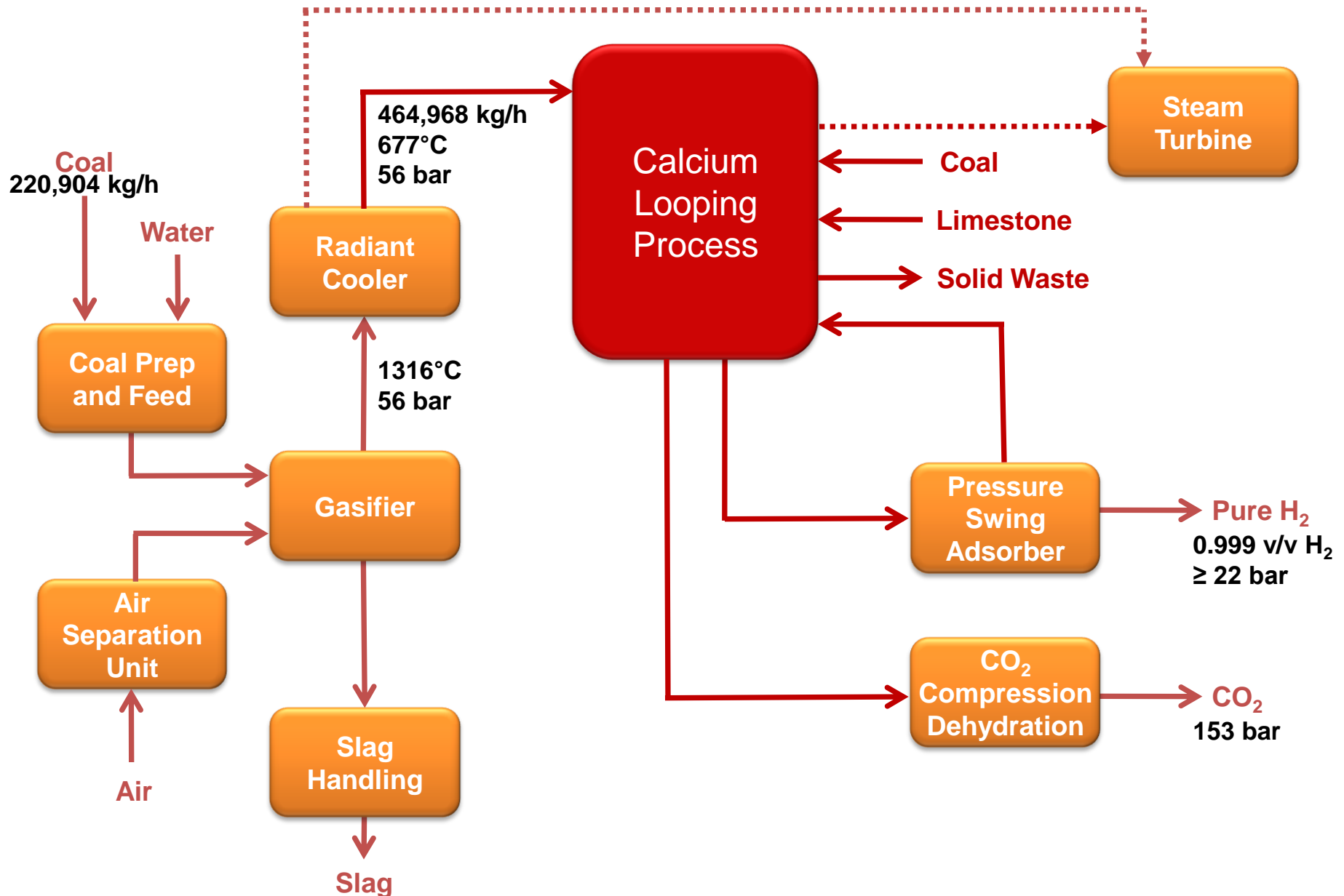


Calcium Looping Sub-pilot Unit for Hydrogen production

Base Coal-to-Hydrogen Process

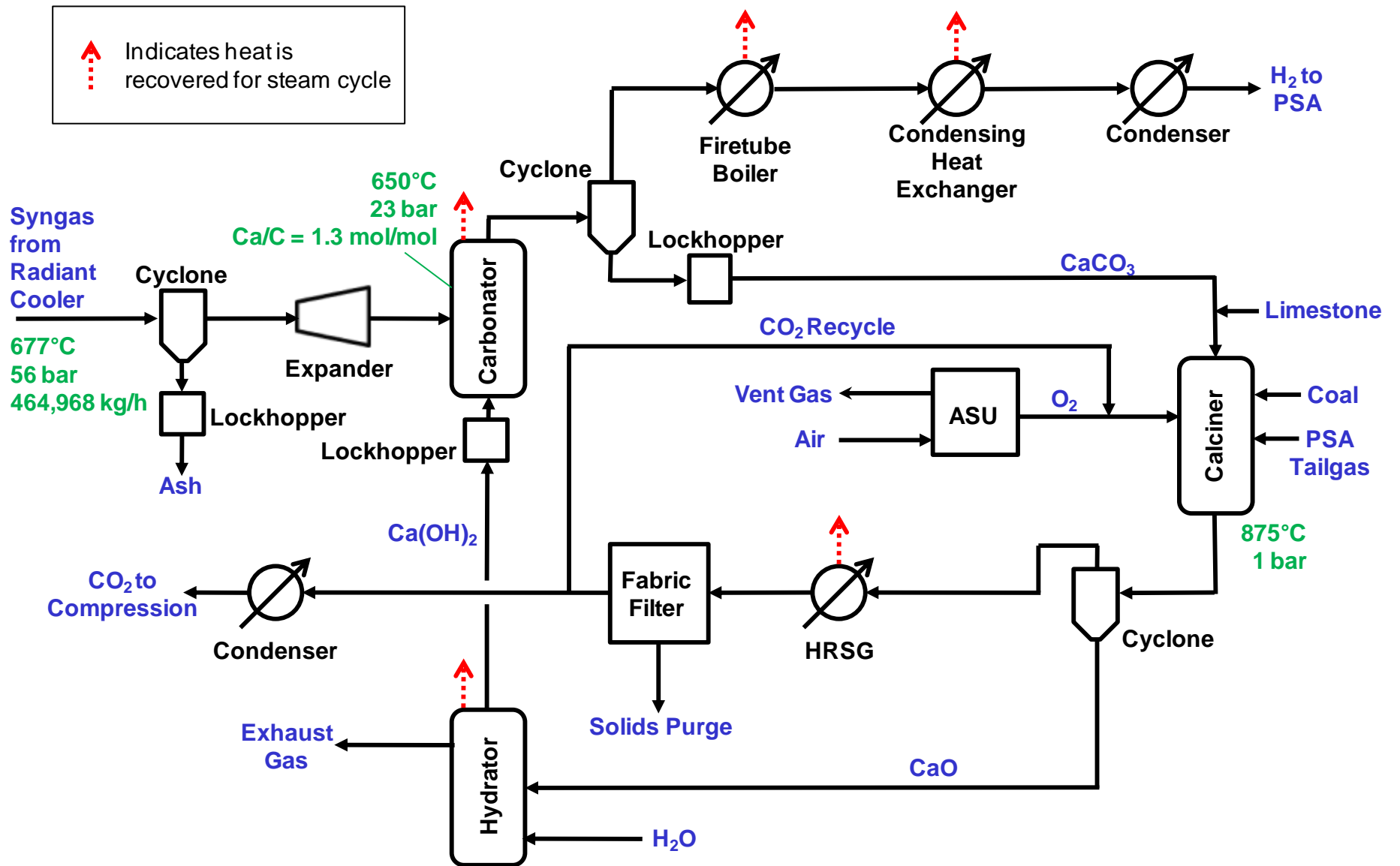


CLP Coal-to-Hydrogen Process



CLP Process Flow Diagram

Coal-to-Hydrogen Plant



Economic Analysis Results

Coal-to-Hydrogen and SMR Cases

	Coal-to-Hydrogen Case		SMR Case	
	Base Plant	CLP Plant	Base Plant	CLP Plant
First-Year Capital (\$/kg)	\$2.26	\$2.58	\$0.62	\$0.96
Fixed O&M (\$/kg)	\$0.43	\$0.57	\$0.16	\$0.26
Fuel (\$/kg)	\$0.36	\$0.55	\$1.22	\$1.40
Electric Power ^a (\$/kg)	-\$0.03	-\$1.13	\$0.14	-\$0.70
CO ₂ Emissions (\$/kg)	\$0.06	\$0.00	\$0.03	\$0.00
Other Variable O&M (\$/kg)	\$0.04	\$0.14	\$0.02	\$0.05
TOTAL FIRST-YEAR COH (\$/kg)	\$3.12	\$2.72	\$2.19	\$1.98
TOTAL FIRST-YEAR COE (\$/MWh)	\$105.00	\$91.61	\$105.00	\$94.91

^aComputed using electricity price equal to the total COE value shown in the table.

$\Delta = -13\%$

$\Delta = -10\%$

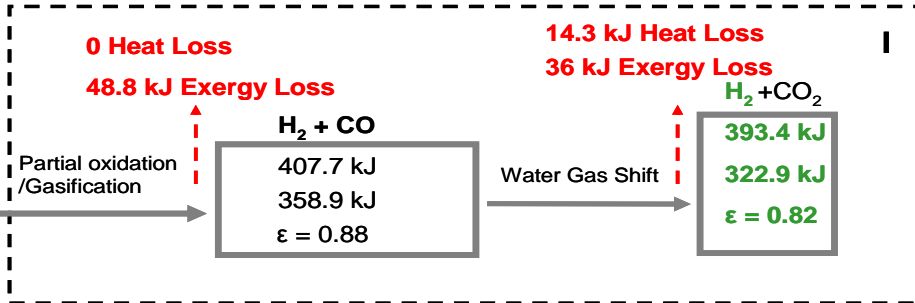
Exergy Analysis on Hydrogen Production

Substance
Enthalpy of degradation
Exergy
Exergy Rate (ϵ)

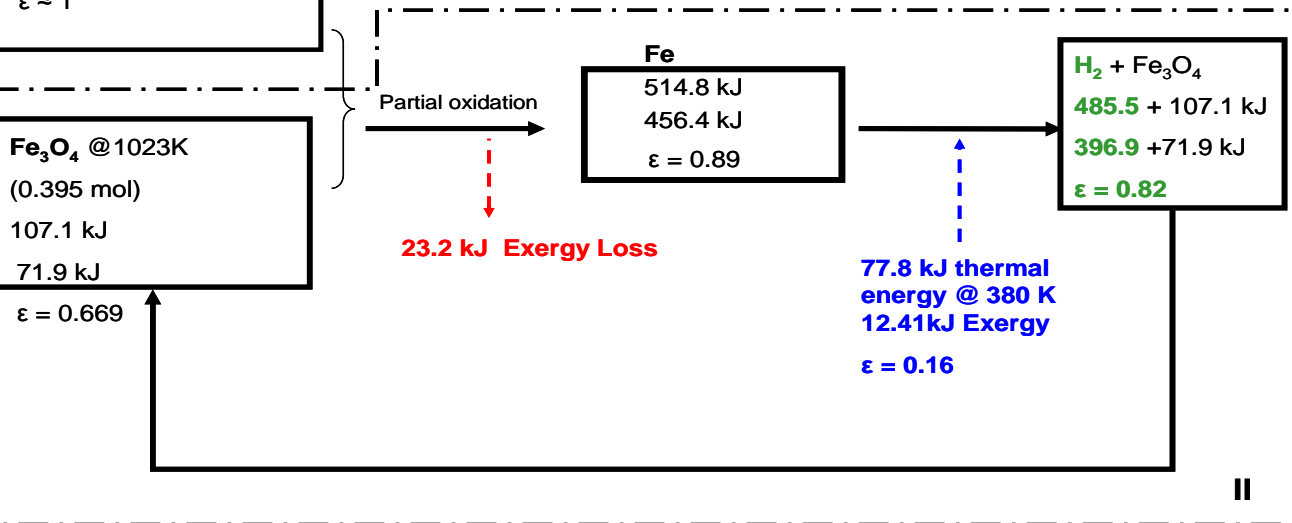
■ Energy/Exergy Loss
■ Additional Energy Input
■ Final Product

Carbon
407.7 kJ/mol
407.7 kJ/mol
 $\epsilon \approx 1$

Fe₃O₄ @ 1023K
(0.395 mol)
107.1 kJ
71.9 kJ
 $\epsilon = 0.669$



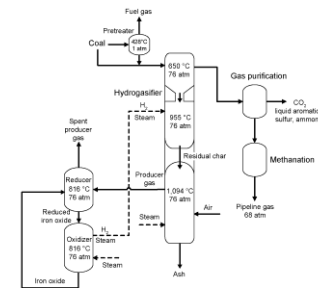
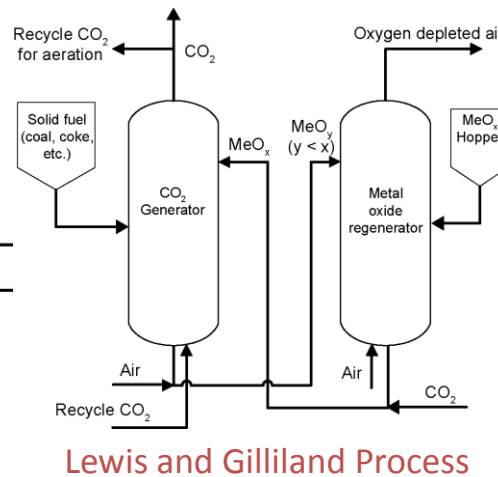
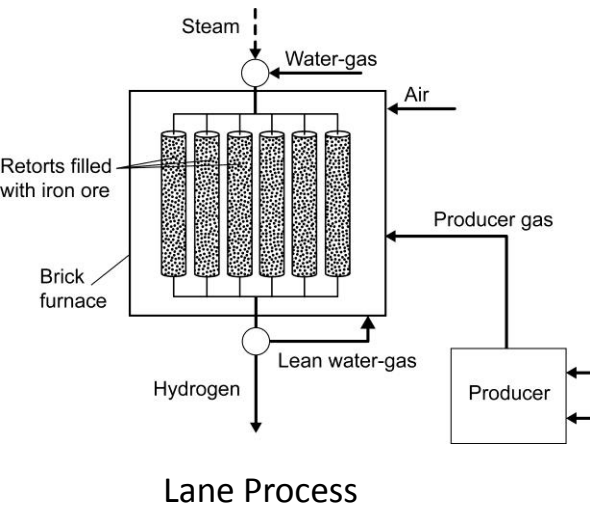
I. Contional Process
Exergetic Efficiency
 $322.9/407.7 = 79.2\%$



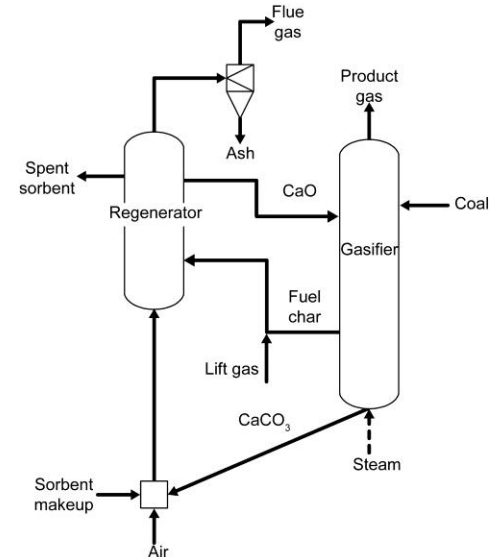
II. Chemcial Looping Process
Exergetic Efficiency
 $396.9/(407.7 + 12.41) = 94.5\%$

Historical Development of Chemical Looping Technologies for Fossil Energy Conversions

Technologies	Lane Process and Messerschmitt Process	Lewis and Gilliland Process	IGT HYGAS Process	CO ₂ Acceptor Process
Time	Early Twentieth Century	1950s	1970s	1970s
Looping Media	Fe/FeO/Fe ₃ O ₄	Cu ₂ O/CuO	FeO/Fe ₃ O ₄	CaO/CaCO ₃
Reactor Design	Fixed bed	Fluidized bed	Staged fluidized bed	Fluidized bed



IGT Process



CO₂ Acceptor Process

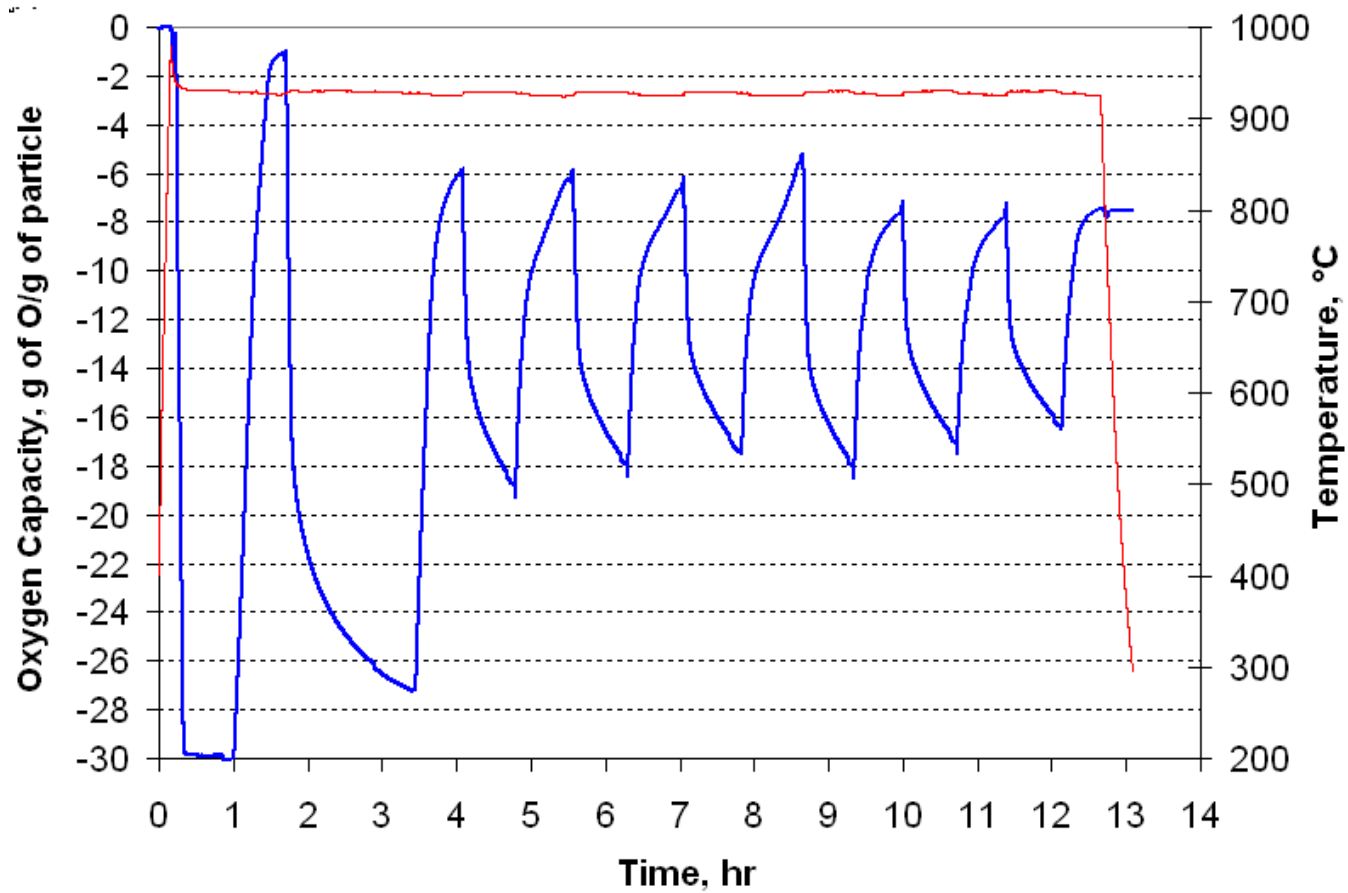
IGT Steam Iron HYGAS Process

	MO=> M	M=> MO
Gas Conversion (%)	65	45
Solid inlet	80% Fe ₃ O ₄ - 20% FeO	95% FeO- 5% Fe
Temperature (°C)	900	900
Reactor	Fluid Bed	Fluid Bed

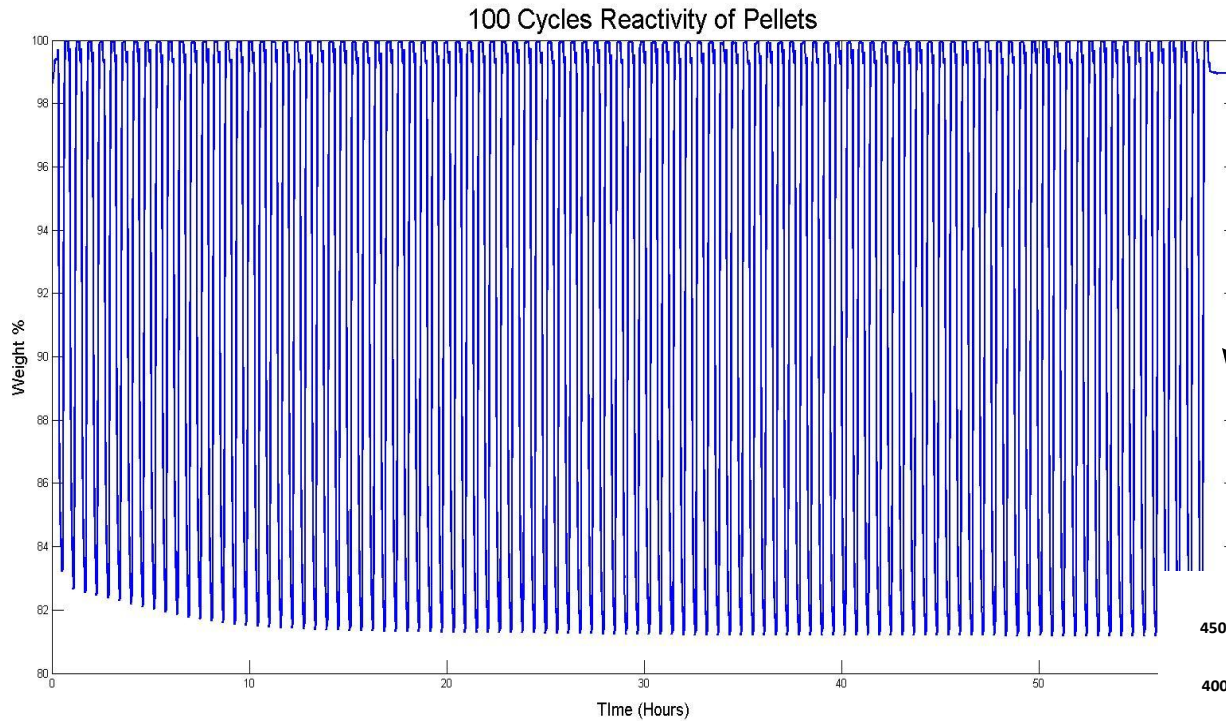
- Poor solid phase conversions: Used only about 25% oxygen capacity of the particles.
- Low gas phase conversions:
- Used iron ore: Low reaction rates
- Only about 40% efficient
- The process not geared towards making pure CO₂

Poor Thermo

Recyclability of Commercial Fe_2O_3

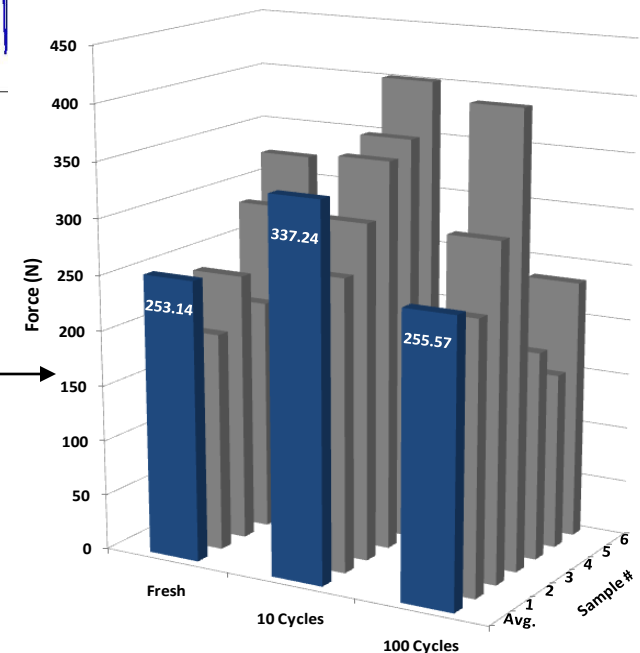


Performance of Composite Fe_2O_3



100 Cycle Pellet Reactivity

100 Cycle Pellet Strength

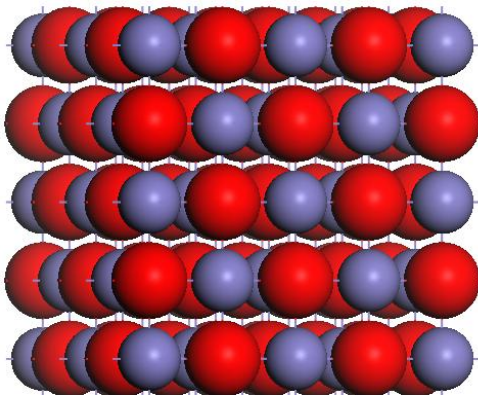


Oxygen Carrier Selection

Primary Metal	Fe	Ni	Cu	Mn	Co
Potential Supports	Al_2O_3 , TiO_2 , MgO , Bentonite, SiO_2 , etc				
Cost	+	—	—	~	—
Oxygen Capacity ¹ (wt %)	30	21	20	25 ³	21
Thermodynamics for CLC	+	~	+	+	+
Kinetics/Reactivity ²	—	+	+	+	—
Melting Points	+	~	—	+	+
Strength	+	—	~	~	~
Environmental& Health	~	—	—	~	—
Hydrogen Production	+	—	—	—	—

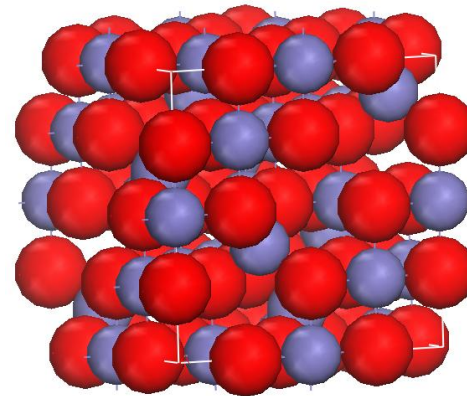
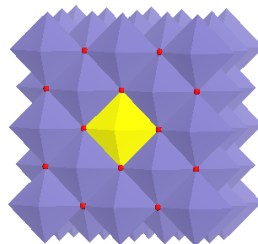
1. Maximum theoretical oxygen carrying capacity; 2. Reactivity with CH_4 ; 3. Mn_3O_4 is the highest oxidation state based on thermodynamics, although not thermodynamically favorable, Mn is assumed to be the lowest oxidation state

Structures of Iron Oxide



NaCl Type

- **oxygen** close-packed cubic pattern
- **iron** occupy all **octahedral** interstices



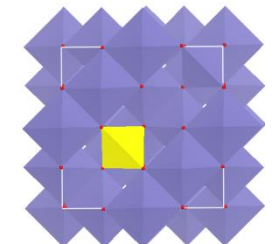
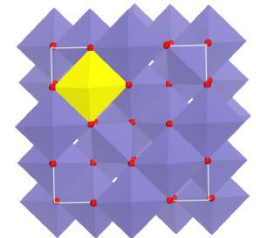
inverse Spinel Type

octahedral interstices

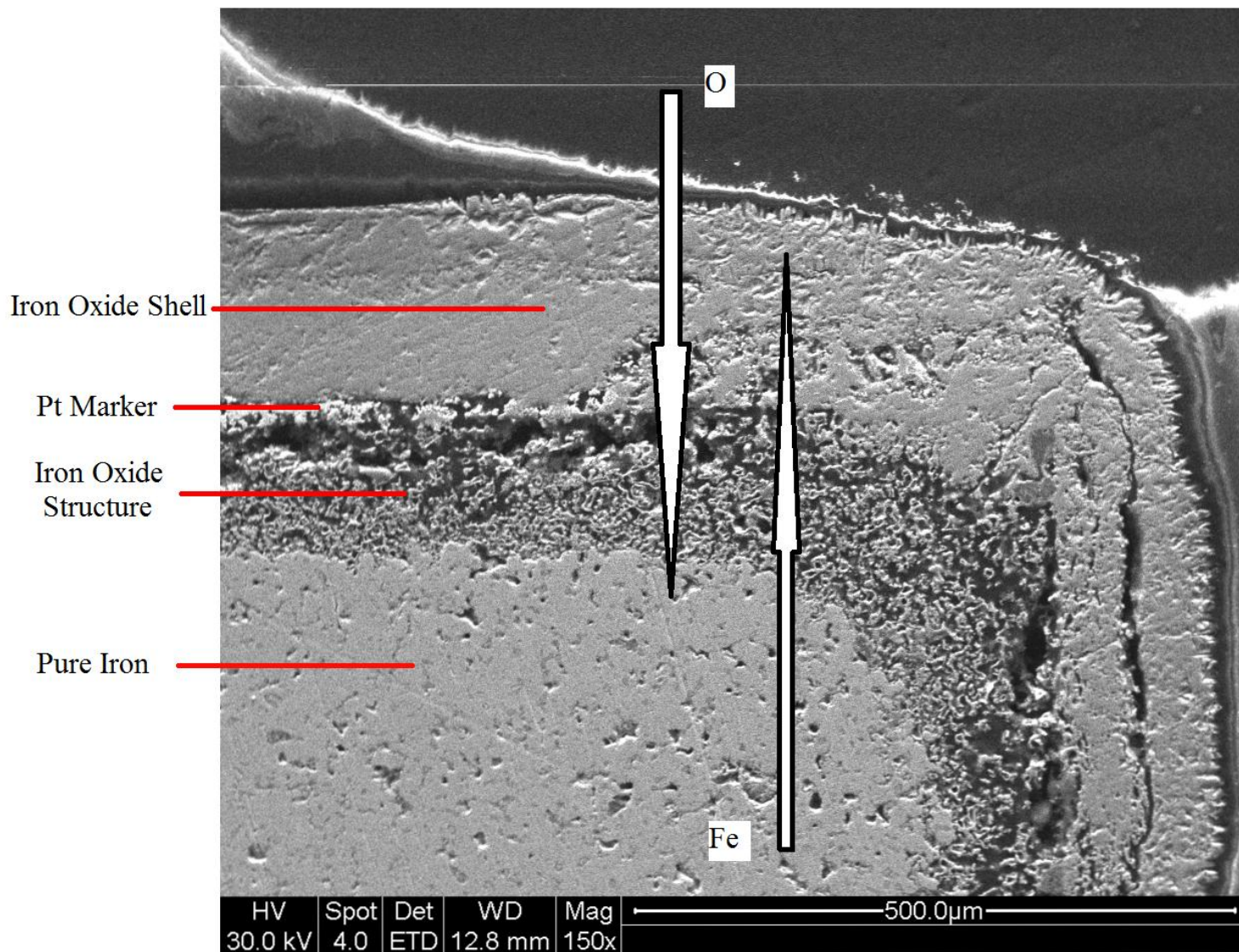
1/2 occupation rate

tetrahedral interstices

1/8 occupation rate

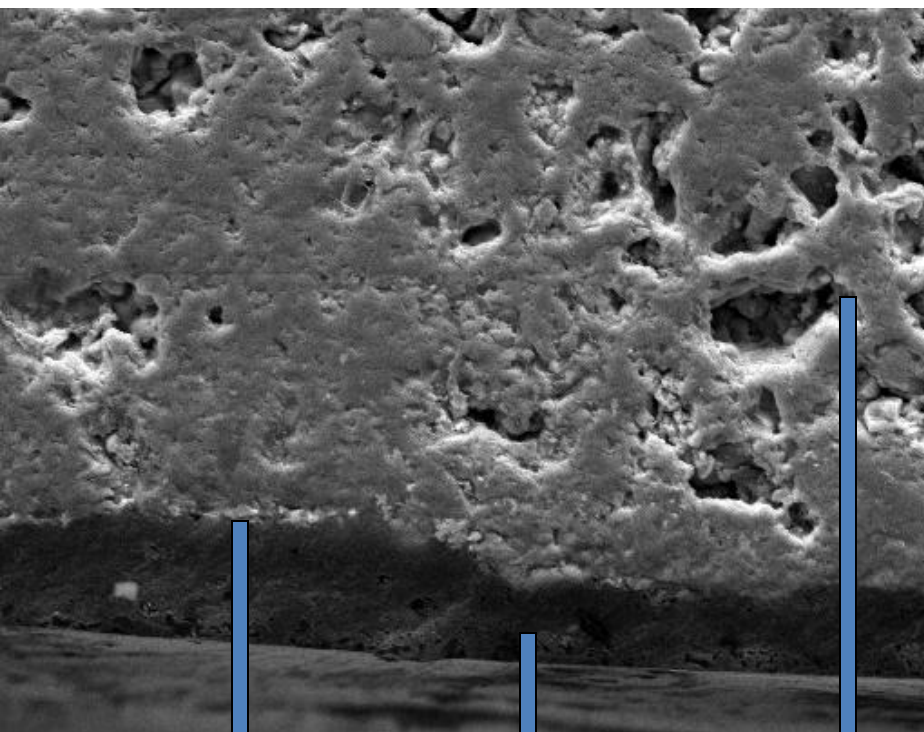


Pellet Reaction Mechanism – Ionic Diffusion for Unsupported Iron



Pellet Reaction Mechanism – Ionic Diffusion for Supported Iron

Partially oxidized Fe with support

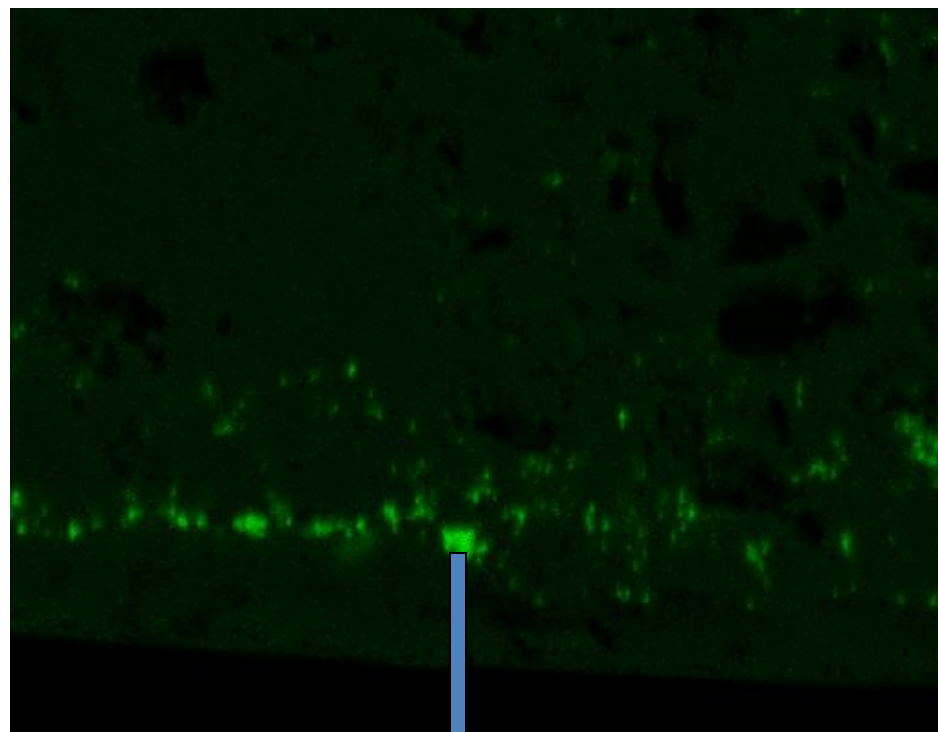


Pt

Epoxy Resin

Pellet bulk phase

Pt mapping

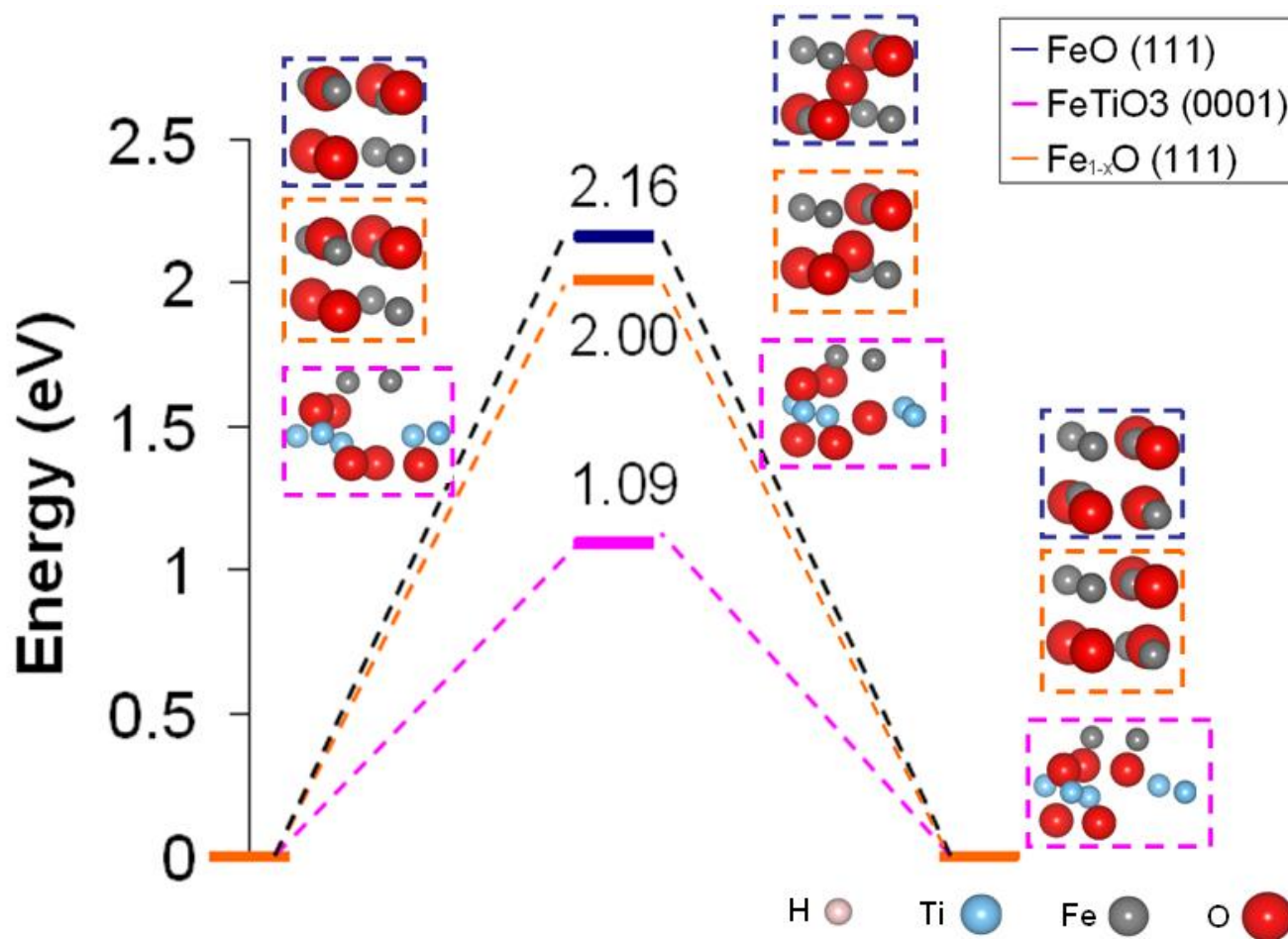


Pt

Role of Support – Oxidation of Fe and Fe/TiO₂

Simulation

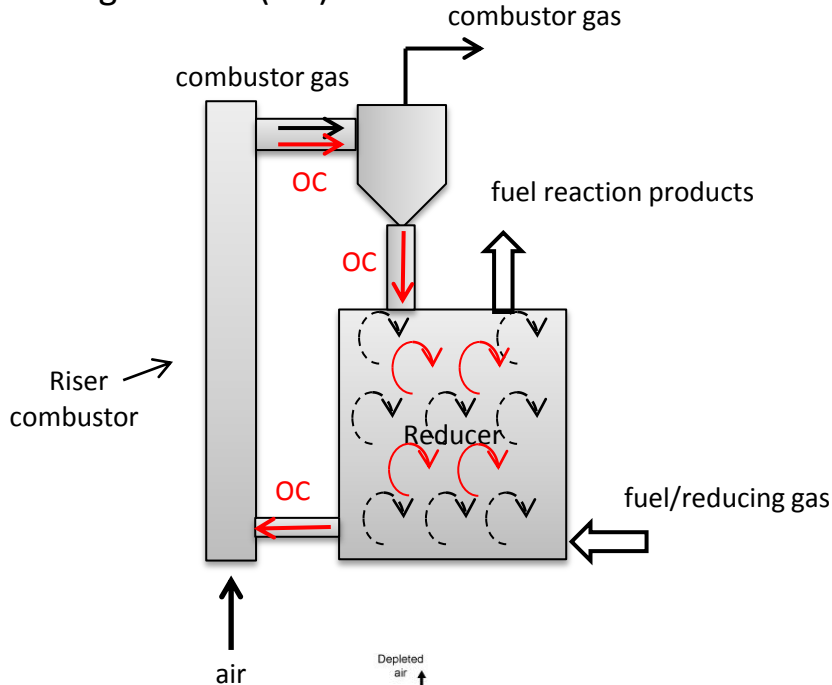
Oxygen anion transfer in Wüstite and Ilmenite



Energy barrier for O²⁻ can be reduced after support addition

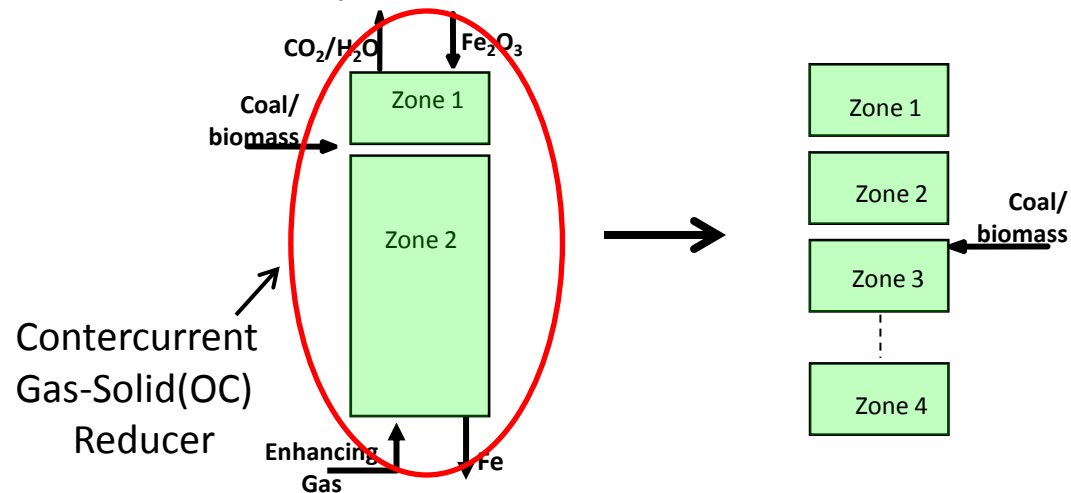
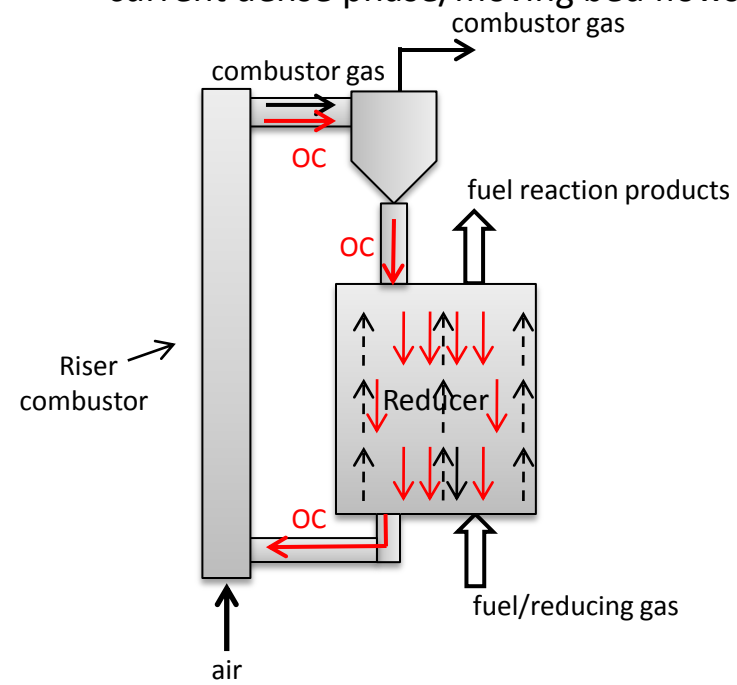
Modes of CFB Chemical Looping Reactor Systems

Mode 1- reducer: fluidized bed or co-current gas-solid (OC) flows



Fluidized Bed Reducer

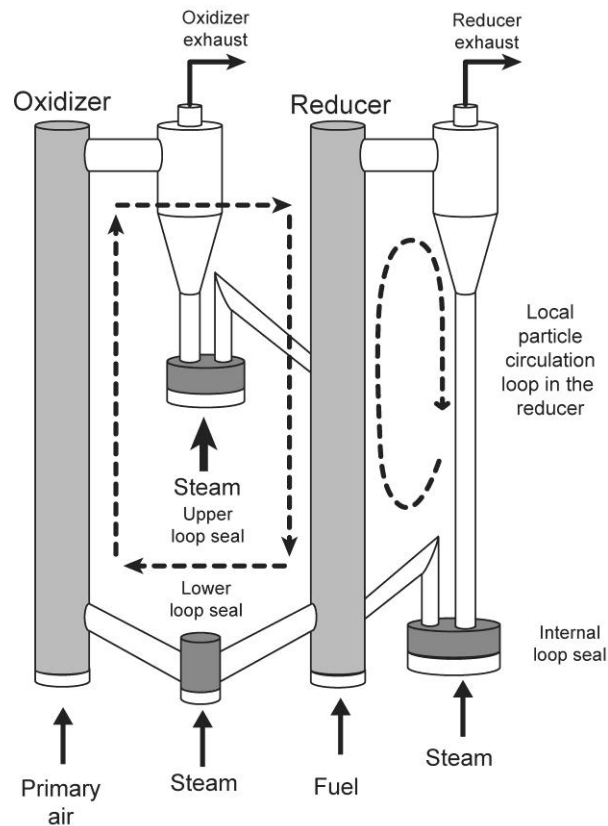
Mode 2 - reducer: gas-solid (OC) counter-current dense phase/moving bed flows



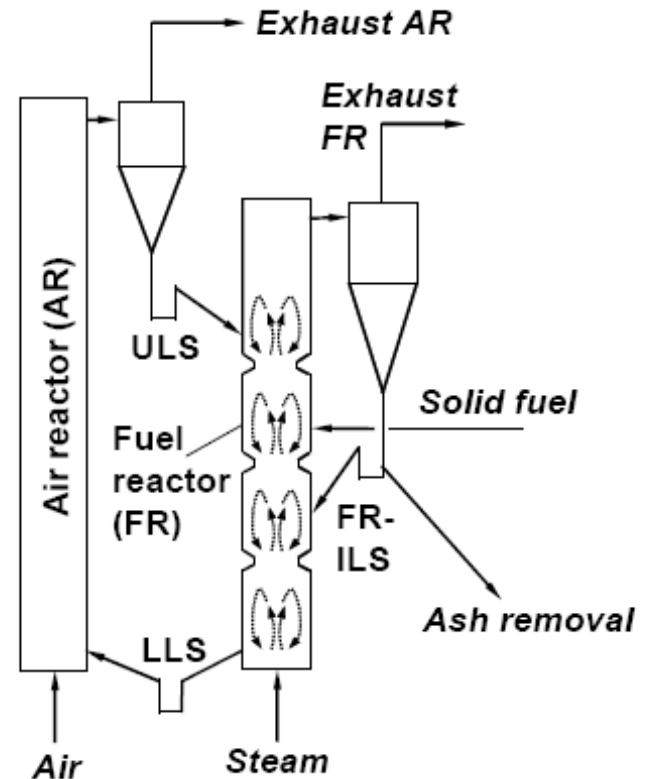
Contercurrent Gas-Solid(OC) Reducer

Design Variation from Mode 1 to Mode 2

Original VUT 120-kW_{th} CLC System
(2007)

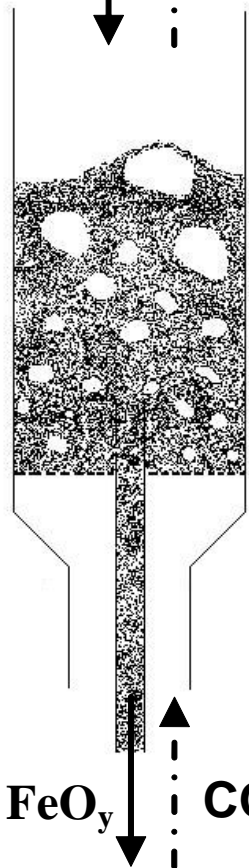


Modified VUT 120-kW_{th} CLC System
(2010)



Chemical Looping Reactor Design

FeO_x ↓ ↑ $\text{CO}_2/\text{H}_2\text{O}$



Fluidized Bed

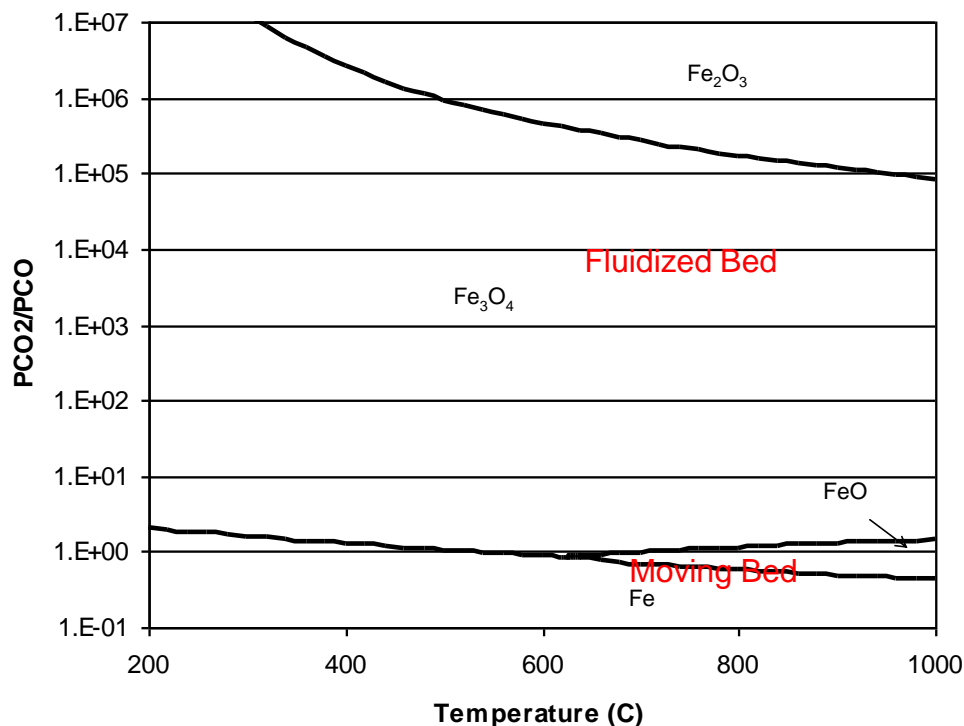
$(x > y)$

Fluidized Bed v.s. Moving Bed

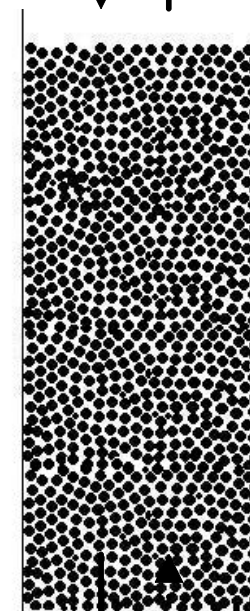
11.11% ← Maximum Solid Conversion → 50.00%

$> U_{mf}$ ← Gas Velocity → $< U_{mf}$

Small ← Particle Size → Large



FeO_x ↓ ↑ $\text{CO}_2/\text{H}_2\text{O}$

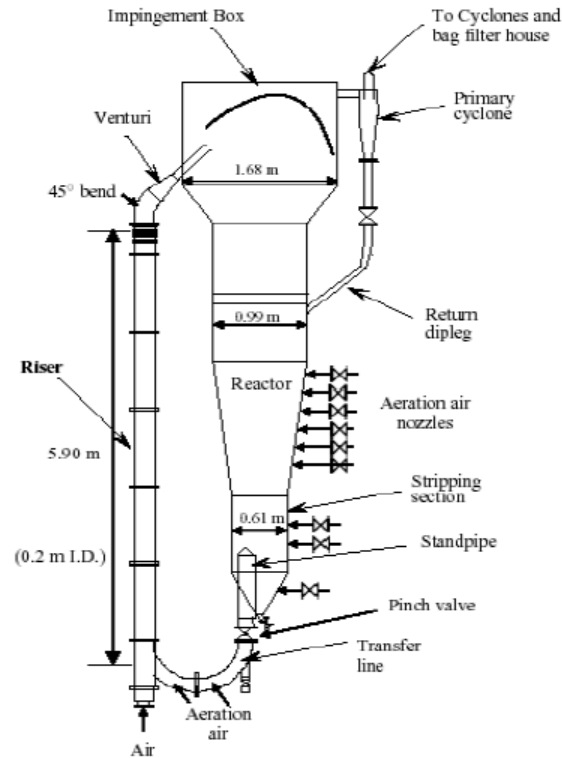


FeO_y ↓ ↑ CO/H_2

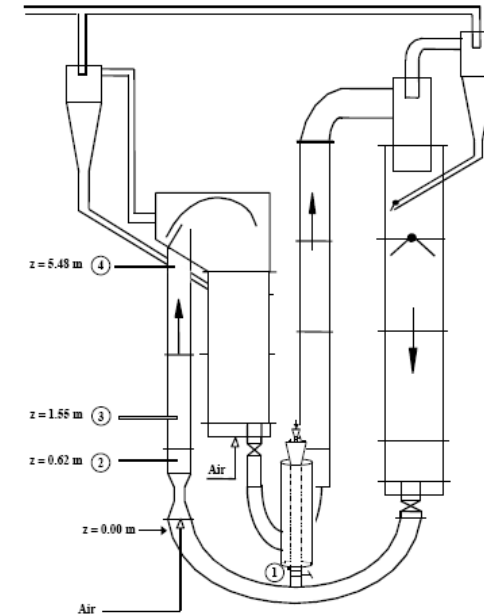
Moving Bed

Particle Type	Ni		Cu		< 3,000 ton/hour		
Type of Data	Lab	CFB 120	Lab		300W	25 kW	
Particle Type	NiO/ MgAl ₂ O ₄	NiO/ MgAl ₂ O ₄	CuO/ Al ₂ O ₃	CuO/Al ₂ O ₃	Fe ₂ O ₃ / MgAl ₂ O ₄	Fe ₂ O ₃ / Al ₂ O ₃	Composite Fe ₂ O ₃
Air Flow Rate @1000 MWth and 10% Excess (mol/s)	11784						1309
Volumetric Air Flow Rate at 1 atm and 900 °C (m ³ /s)	1134						126
Particle Circulation Rate @ 1000 MWth (kg/s)	4000	10000	3000	6000	8000	10000	800
Reducer Solids Inventory (tonne)	230	160	70	total 2100	500	1200	1500 Total
Oxidizer Solids Inventory (tonne)	390	80	390		n/a	350	
Medium Particle Size (µm)	153	120	300	200	153	151	2000
Particle Density (g/cm ³)	1.9	5	2.5	2.5	4.1	2.15	2.5
Ut (m/s)	2	0.8	2	1.2	1.1	0.6	11
Uc (m/s)	4	4.8	4.9	4.2	4.8	3.6	4
Use (m/s)	6	6.7	7.5	6.1	6.9	4.9	9.7
Typical Riser Superficial Gas Velocity (m/s)	7.00						12
Bed Area Turbulent Section (if Required) at 1 atm (m ²)	231.47						25.18
Bed Area Required for Riser Section at 1 atm (m ²)	162.03						10.49
Corresponding Riser Diameter (m)	14.37						3.66
<i>Solids Flux</i> at 1 atm (kg/m ² s)	24.69	61.72	18.52	37.03	49.37	61.72	76.23
Number of Beds Needed given 8 m ID Riser	3.23						<1
Number of Beds Needed given 1.5 m ID Riser	91.73						5.94
Ug for a Single 1.5 m ID Riser at 1 atm (m/s)	642.14						71.29
Ug for a Single 8 m ID riser at 1 atm (m/s)	22.58						2.5 (Ug < Ut; N/A)
Required Pressure for a Single 1.5m ID Riser (atm)	91.73						10.00
<i>Solids Flux</i> for a Single 1.5 m ID Riser (kg/m ² s)	2264.69	5661.71	1699	3397.03	4529.37	5661.71	452.88
Required Pressure for a Single 8 m ID Riser (atm)	3.23						26 Ug < Ut; N/A
<i>Solids Flux</i> for a Single 8 m ID Riser (kg/m ² s)	79.62	199.04	59.71	119.43	159.24	199.04	

Circulating Fluidized Bed Systems



Single Loop High Density CFB System
(Kirbas et al., 2007)



Two Loop High Density CFB System (Kulah et al., 2008)

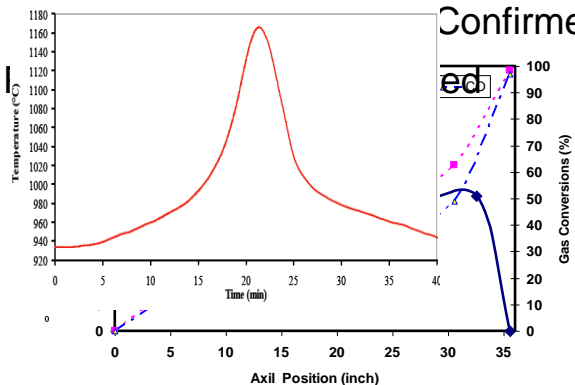
Kirbas G, Kim SW, Bi X, Lim J, Grace JR. Radial Distribution of Local Concentration Weighted Particle Velocities in High Density Circulating Fluidized Beds. Paper presented at: The 12th International Conference on Fluidization - New Horizons in Fluidization Engineering; May 13-17, 2007; Vancouver, Canada.

Kulah G, Song X, Bi HT, Lim CJ, Grace JR. A NOVEL SYSTEM FOR MEASURING SOLIDS DISPERSION IN CIRCULATING FLUIDIZED BEDS. Paper presented at: 9th International Conference on Circulating Fluidized Beds; May, 13 – 16, 2008; Hamburg, Germany.

OSU Syngas Chemical Looping Process Development

Maximum Operating Temperature Determined

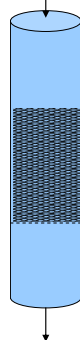
Confirmed



Scale



Particle



Fixed Bed Tests



Bench Scale Tests

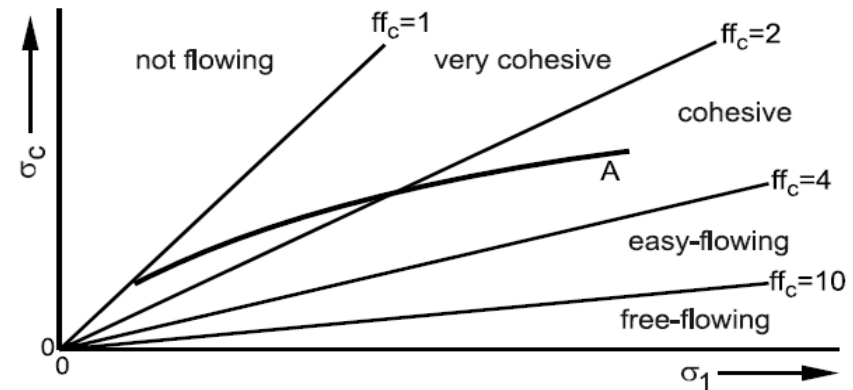
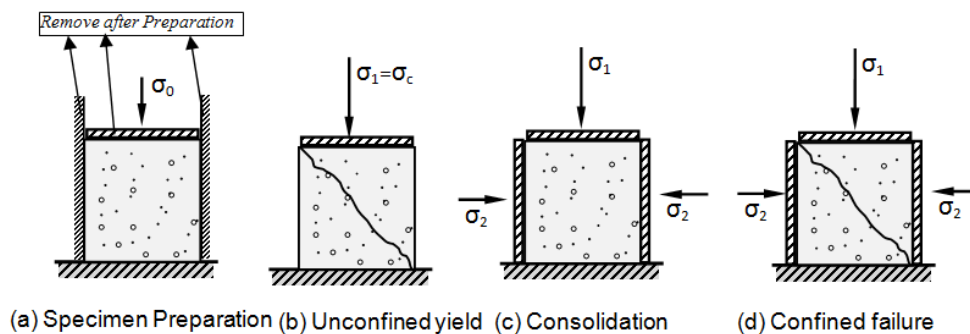
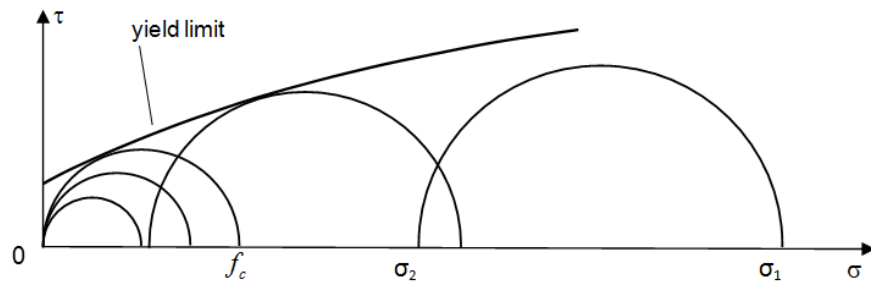


Sub-Pilot SCL
Integrated Tests

Time



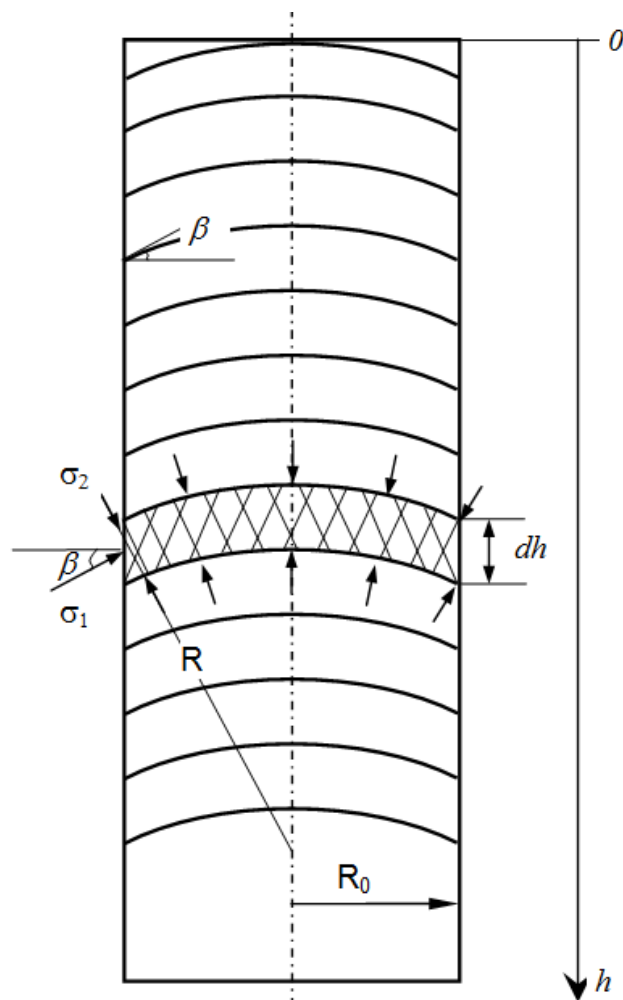
Flow Properties of Bulk Solids



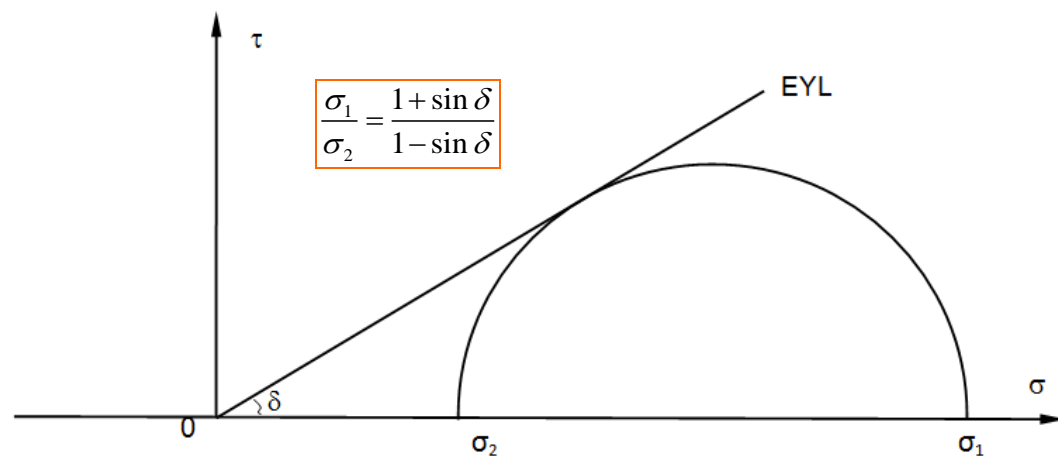
$$ff_c = \frac{\sigma_0}{f_c} : \text{flowability of bulk solids}$$

Consolidation and Yield of Bulk Solids

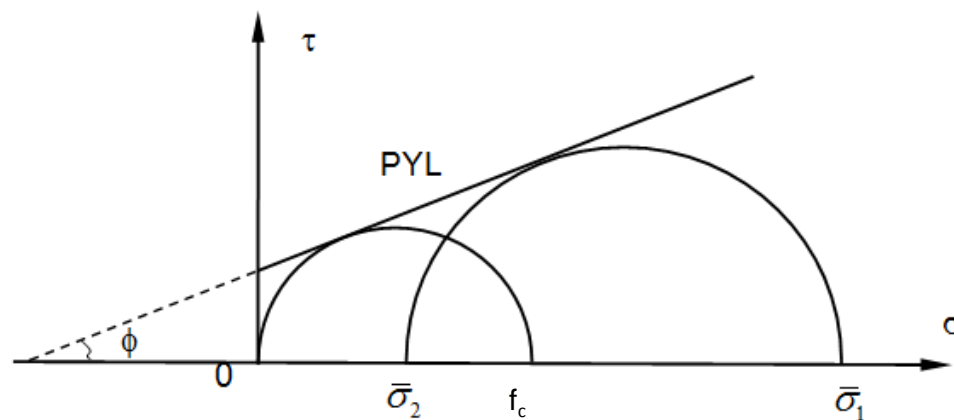
Stress of Bulk Solids in Vertical Reactor



Piling of Bulk Solids



Flowing Condition



Arching Condition

Stress Condition of Bulk Solids

Stress Distribution in Flowing Solids

Limitation from wall: fully developed wall angle

$$\tau_{xy} = \frac{\sigma_1 + \sigma_2}{2} \sin \delta \sin 2\beta = \frac{\sigma_1 + \sigma_2}{2} (1 + \sin \delta \cos 2\beta) \tan \varphi$$

φ : angle of friction between the powder and the wall

$$\sin(2\beta - \varphi) = \frac{\sin \varphi}{\sin \delta} = \sin \nu$$

$$\Rightarrow \beta = \frac{\nu + \varphi}{2}$$

$$\Delta W = \Delta F_{\text{lift}} + \Delta F_{\text{upward}}$$

$$\Delta W = \pi R_0^2 \Delta h \rho_s g$$

$$\Delta F_{\text{support}} = \pi R_0^2 \Delta \sigma_2$$

$$\Delta F_{\text{lift}} = \pi R \Delta h (\sigma_1 - \sigma_2) \sin 2\beta$$

$$\rho_s g = \frac{2 \sin \delta \sin 2\beta}{R_0 (1 - \sin \delta)} \sigma_2 + \frac{d\sigma_2}{dh}$$

$$\begin{cases} a = \frac{2 \sin \delta \sin 2\beta}{R_0 (1 - \sin \delta)} \\ b = \frac{R_0 (1 - \sin \delta)}{2 \sin \delta \sin 2\beta} \rho_s g \end{cases}$$

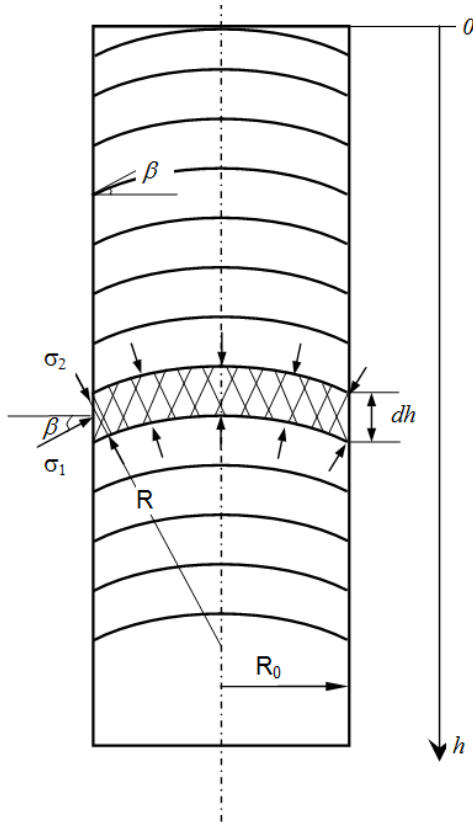
$$\sigma_2 = b + (\sigma_0 - b)e^{-ah}$$

σ_0 : external normal stress at the top of the solid surface

With counter-current interstitial gas flow

Drag force can be treated as a reduction of gravity

$$b = \frac{R_0 (1 - \sin \delta)}{2 \sin \delta \sin 2\beta} (\rho_s g - F_D)$$



Reactor Size Criteria for Arching

- No External Stress on Top

$$\bar{\sigma}_2 = b(1 - e^{-ah})$$

$$b = 0 \Rightarrow \frac{R_0(1 - \sin \phi)}{2 \sin \phi \sin 2\beta'} \rho_s g = \frac{f_c(1 - \sin \phi)}{2 \sin \phi}$$

$$R_0 \geq \frac{f_c \sin 2\beta'}{\rho_s g}$$

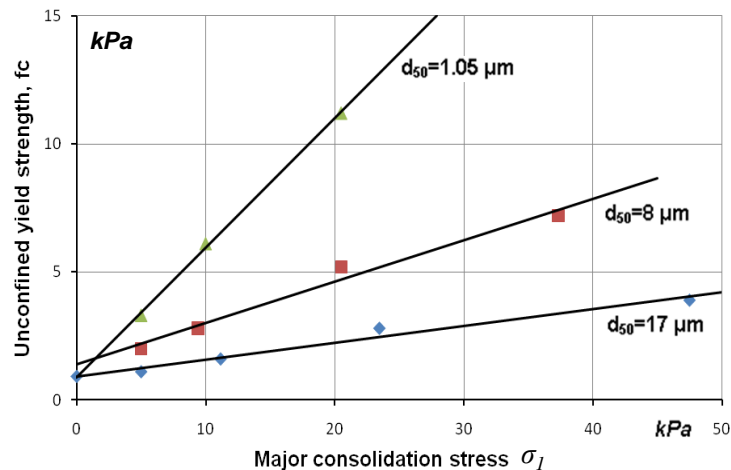
Influence of Some Critical Parameters

1. Gas Flow

$$R_0' \geq \frac{f_c \sin 2\beta'}{\rho_s g - F_D} > R_0$$

Counter-Current Interstitial gas flow causes reduction of gravity, and thus needs a larger reactor size

2. Particle Size



unconfined yield strength of some alumina-powders (*)

$$R_0' \geq \frac{f_c \sin 2\beta'}{\rho_s g}$$

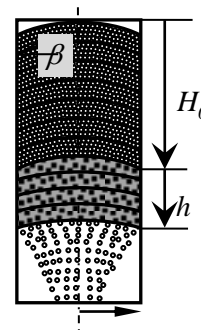
$$f_c \propto \frac{1}{d_p^n}$$

Smaller particles need
larger reactor size

3. Mixing with Fine Powders

The flowability governed by flow properties of the fine powders as shearing takes place across the fines.

4. Layer of Fine Powders

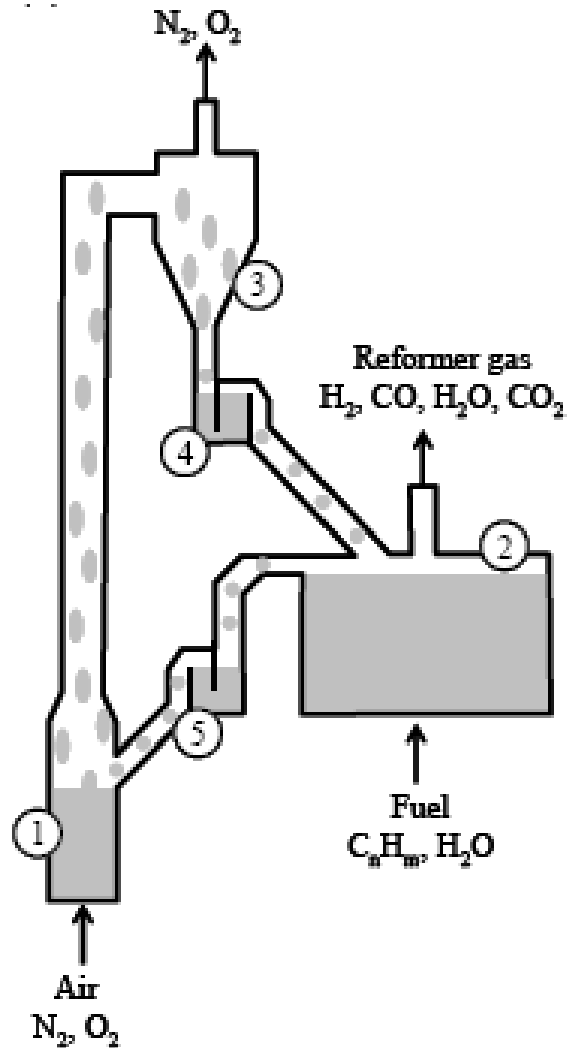


Arching Criteria:

depend on height of fine powder layer

$$h = -\frac{1}{a'} \ln \frac{b'}{b' - \bar{\sigma}_0'}$$

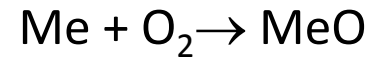
European Chemical Looping Reforming/Gasification Application - I



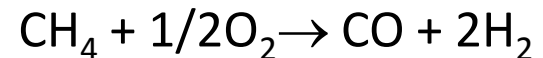
Reducer:



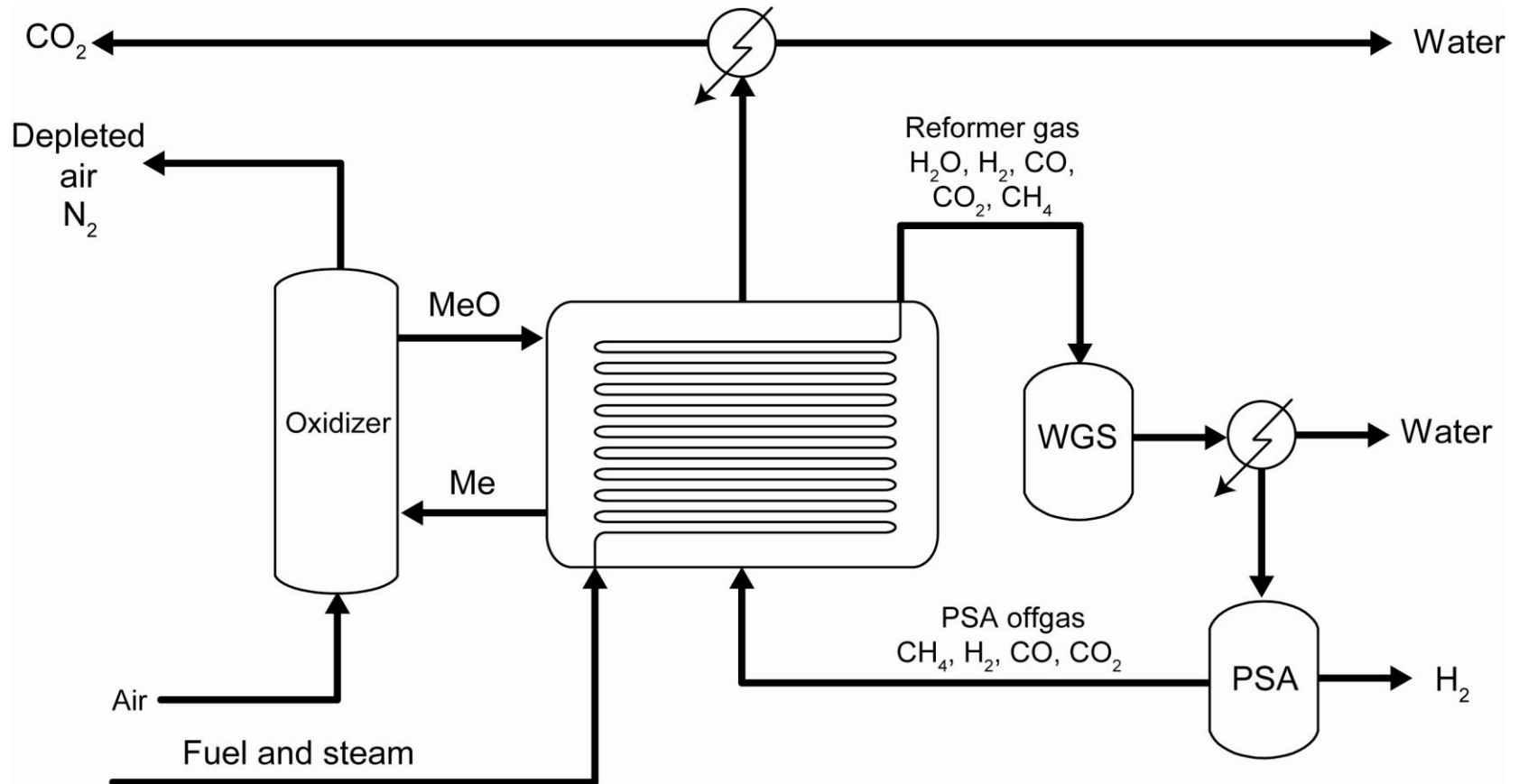
Oxidizer:



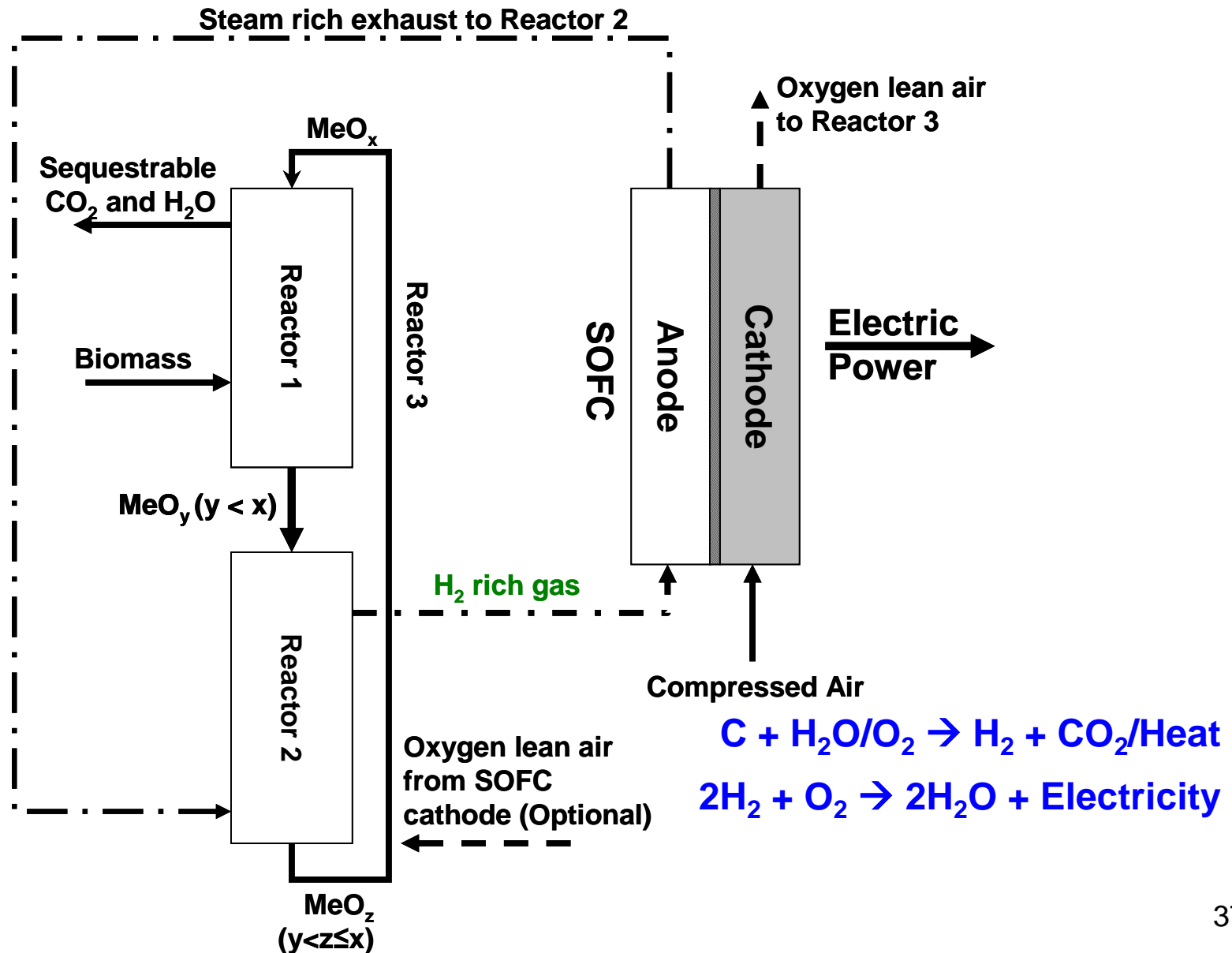
Overall Reaction:



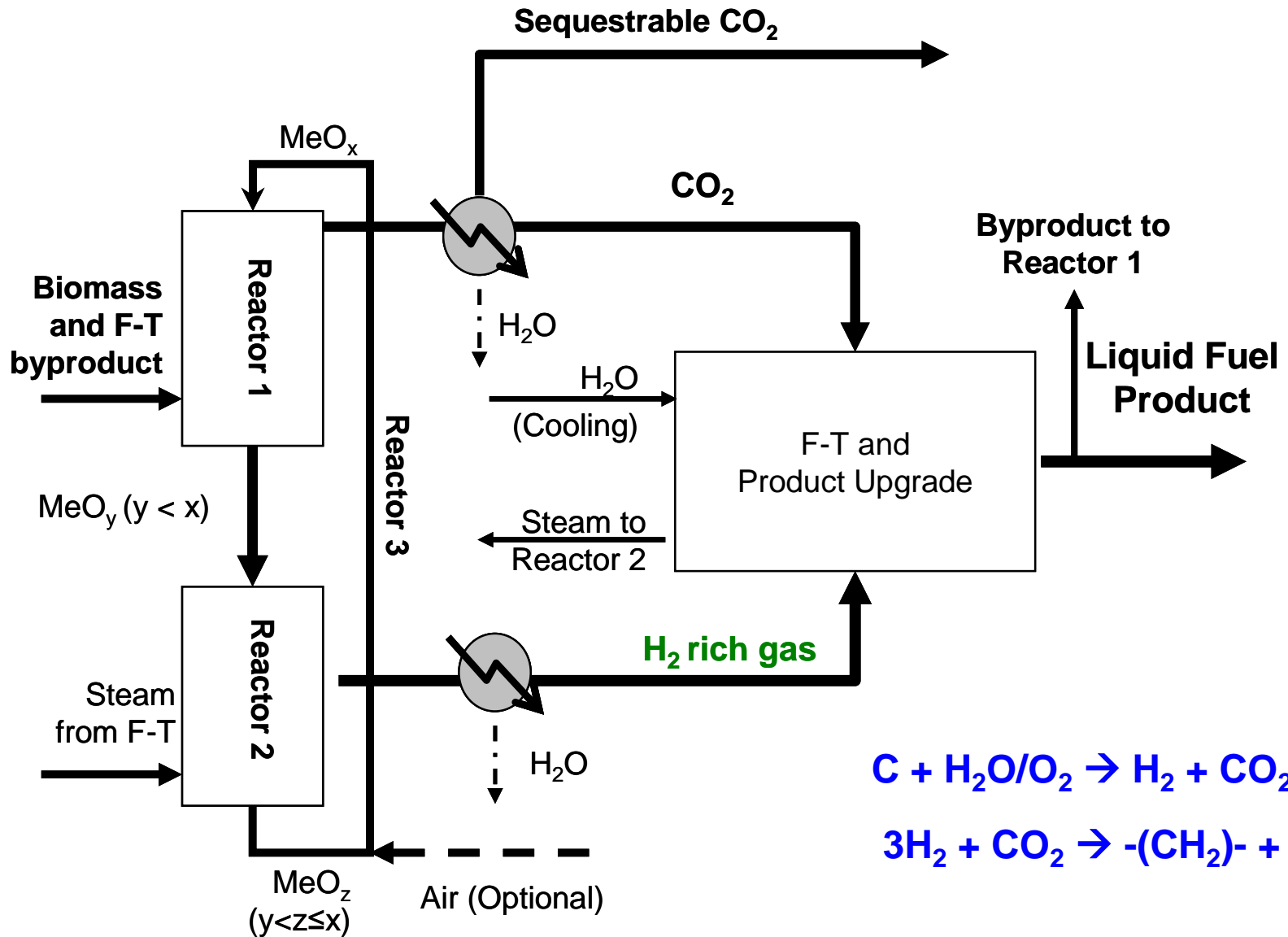
European Chemical Reforming/Gasification Application - II



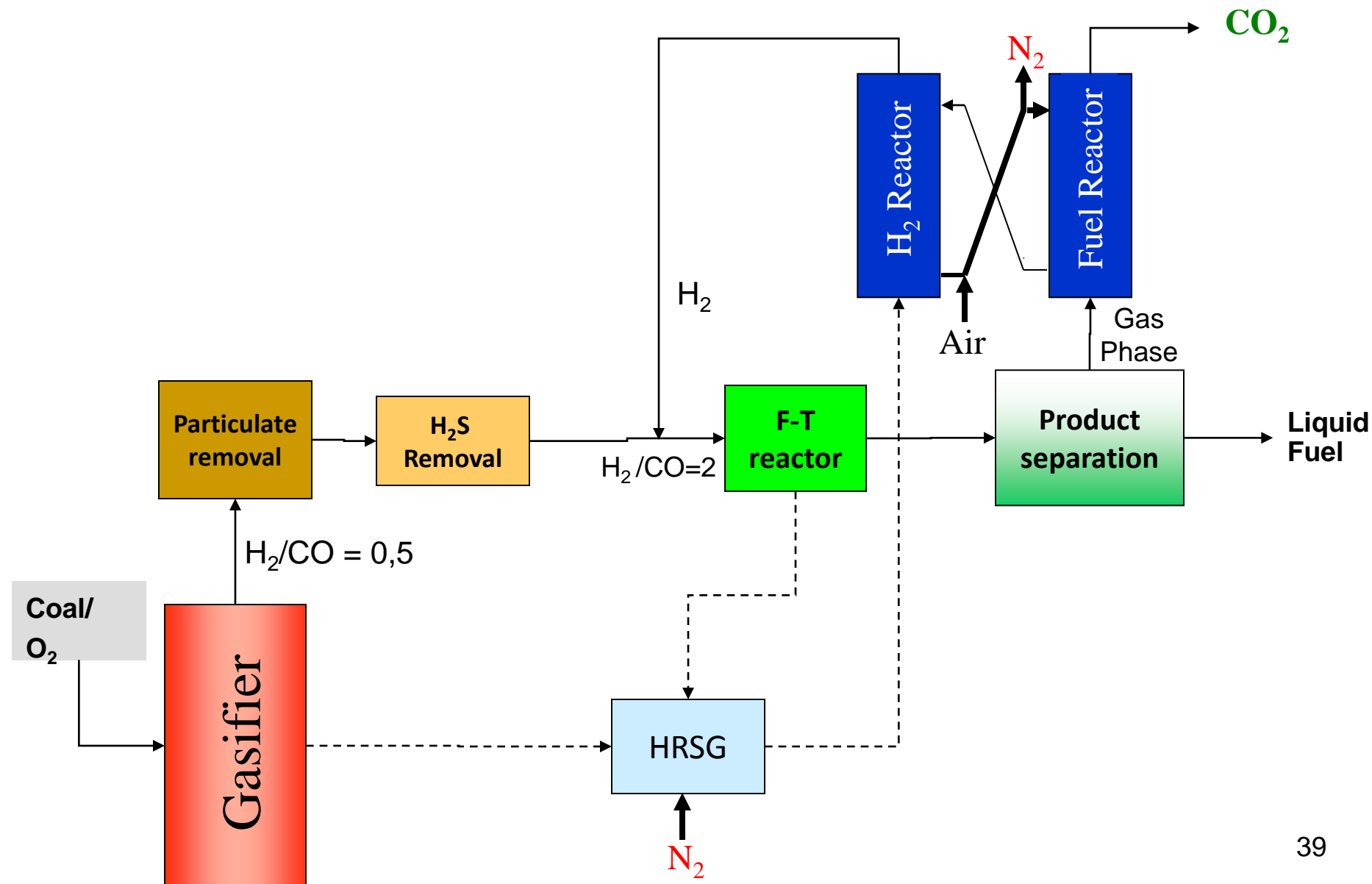
OSU Chemical Looping Integrated with Fuel Cell Application – 3



OSU Syngas Chemical Looping in CTL Applications – II



OSU Syngas Chemical Looping in CTL Applications – I



Upcoming large-scale demonstrations of chemical looping technology

Organization/Location	Process	Size	Features
HUNOSA, Spain	$\text{CaCO}_3 - \text{CaO}$ (CaOling) looping for post combustion CO_2 capture	2 MWth	CO_2 is from the flue gas generated from 50 MWe coal power plant .
Technical University of Darmstadt, Germany	$\text{CaCO}_3 - \text{CaO}$ (LISA) looping for post combustion CO_2 capture	1 MWth	Capture plant is an extension to a 1052 MWe hard coal-fired power plant; carbonator and calciner both are CFBs.
Technical University of Darmstadt, Germany	ECLAIR – ilmenite Redox with coal for looping combustion application	1 MWth	Solid fuel conversion uses a fluidized bed reducer operated in a CFB looping system
Alstom, U.S.	$\text{CaCO}_3 - \text{CaO}$ looping for CO_2 capture / $\text{CaSO}_4 - \text{CaS}$ redox with coal for looping combustion application	3 MWth	Process uses two calcium – based loops in a chemical looping system
OSU, U.S.	Iron based oxygen carrier redox with gaseous fuels for H_2 production in a Syngas Chemical Looping (SCL) gasification process	250 kWth	High pressure SCL enables high purity H_2 generation and high purity CO_2 generation using a countercurrent moving bed reactor

Concluding Remarks

- Chemical Looping embodies all elements of particle science and technology - particle synthesis, flow and contact mechanics, gas-solid reaction engineering...
- Success achieved in the operation of sub-pilot units reflect the likelihood of commercialization of this technology in the near future